Advances in wearable flexible piezoelectric energy harvesters: materials, structures and fabrication

Xiaoquan Shi[1, 2], Yazhou Sun[1] *, Dekai Li[1], Haitao Liu[1] *, Wenkun Xie[2], Xichun Luo[2]

[1] Department of Mechanical Engineering and Automation, Harbin Institute of Technology, Harbin 150001, China

[2] Centre for Precision Manufacturing, DMEM, University of Strathclyde, Glasgow G1 1XJ, UK

 *Haitao Liu: hthit@hit.edu.cn

*Yazhou Sun: sunyzh@hit.edu.cn

Abstract

Flexible energy harvesters have become a research hotspot in both academia and industry because of their great advantages in powering wearable electronic devices. The flexible energy harvesters based on piezoelectric materials are recognized as a competitive method because of their sensitivity to mechanical deformation, excellent energy conversion performance, mature production technology and simple structure. This paper presents a comprehensive review to illustrate the research progress and future development of wearable flexible piezoelectric harvesters. In this work, the widely-used piezoelectric materials for flexible energy harvesters, including inorganic piezoelectric materials, organic piezoelectric materials and piezoelectric composites, are first summarized. The research progress on the influence of ceramic content, morphology, distribution, surface chemical modification, and the addition of conductive materials on the properties of piezoelectric composites are systematically discussed. Additionally, this paper also presents novel structures and fabrication methods of flexible piezoelectric energy harvesters.

Finally, future trends in research, development and innovation of flexible piezoelectric energy harvesters are outlined and prospected.

Abbreviations

AC	alternating current
AD	aerosol deposition
BCT	$(Ba,Ca)TiO_3$
BCTZ	$(Ba,Ca)(Ti,Zr)O_3$
BST	$(Ba,Sr)TiO_3$
BT/BTO	$BaTiO_3$
BZT-BCT	$Ba(Zr,Ti)O_3$–$(Ba,Ca)TiO_3$
CNT	carbon nanotube
DC	direct current
DEP	dielectrophoresis
EHD	electrohydrodynamic
FDM	fused deposition modelling
FEH	flexible energy harvester
GA	gallic acid
Ga-ZnO	Ga-doped ZnO
HOG	–OH-functionalized graphene
IoT	Internet of Things
ITO	Indium-tin oxide
KN	$KNbO_3$
KNN/NKN	$(K,Na)NbO_3$
LED	light emitting diode
MWCNT	multi-walled carbon nanotube
NCDS	nanocomposite deposition system
NG	nanogenerator
PBTCA	2-phosphonobutane-1,2,4-tricarboxylic acid

PCL	poly(ε-caprolactone)
PDA	polydopamine
PDMS	polydimethylsiloxane
PEBA	polyether block amine
PEN	polyethylene naphthalate
PET	polyethylene terephthalate
PI	polyimide
PIN-PMN-PT	$Pb(In,Nb)O_3-Pb(Mg,Nb)O_3-PbTiO_3$
PLA	polylactic acid
PLLA	poly(L-lactic acid)
PMMA	poly(methyl methacrylate)
PMN-PT	$Pb(Mg,Nb)O_3-PbTiO_3$
PNN-PZT	$Pb(Ni,Nb)O_3-PbZrO_3-PbTiO_3$
PU	polyurethane
$PVDF/PVF_2$	poly(vinylidenefluoride)
P(VDF-TrFE)	poly(vinylidenefluoride-co-trifluoroethylene)
PZN-PZT	$Pb(Zn,Nb)O_3-Pb(Zr,Ti)O_3$
PZT	$Pb(Zr,Ti)O_3$
RGO	reduced graphene oxide
RF	radio frequency
Tb-ZnO	Tb-doped ZnO
TrFE	trifluoroethylene

1. Introduction

Driven by the rapid development of cloud computing, big data and artificial intelligence (AI), the advent of the Internet of Things (IoT) technologies promises to revolutionize people's lives in different aspects. It is

estimated that 50 billion devices will be interconnected through networks around the world by 2025 [1]. These devices will be widely used in industrial automation production, urban transportation, household, personal health and many more [2-4], as shown in **Figure 1(a)**. Taking healthcare as an example, wearable sensors and their systems including smart watches, smart clothes and other components can be used in the field of human health and environment date real-time collection, preliminary diagnosis of disease, motion recognition and human-machine interaction [5-8], shown in **Figure 1(b)**. However, one key bottleneck for industrial-scale implementation of wearable electronic devices lies in the power supply. Although each device does not require a high energy supply, the use of massive number of sensors will lead to a huge energy consumption. Moreover, these devices are widely distributed and usually require sustainable power supply. The use of conventional batteries will hinder the miniaturization of the equipment, and the production, recycling and disposition of the battery will easily cause environmental pollution [9, 10].
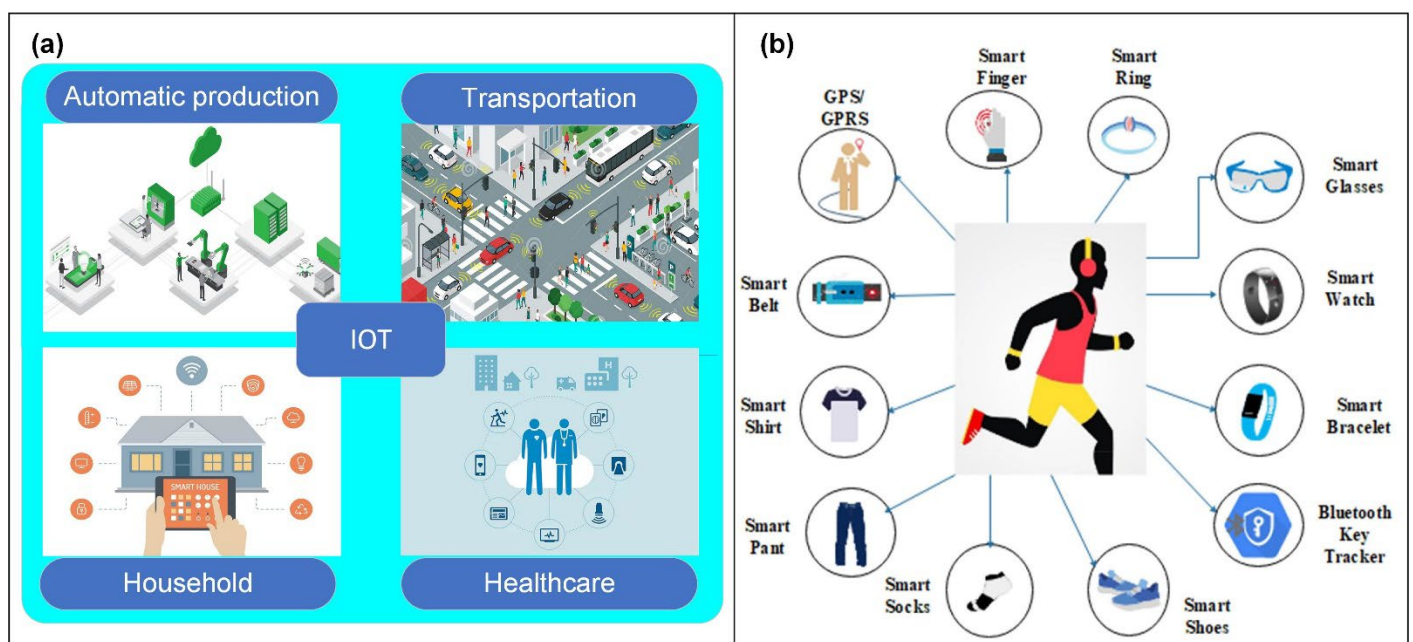

Figure 1. (a) Application of IOT in different fields; (b) IOT equipment for human healthcare [8]

Self-powered technology provides a solution for the energy supply of portable and wearable sensor systems. The self-power technology is designed by using energy harvesters to convert other kinds of energy to electrical energy, which can be realised through two modes: one is to power the sensor systems by harvesting energy from environment or human body; the other one is to convert signal induced by the physical or chemical

5

changes in the environment or human body to electrical signals directly for further analyse [11, 12]. As the energy is usually produced in nano scale, energy harvesters are also called nanogenerators (NGs) [13, 14].

Different kinds of clean and renewable energy in nature, including solar energy, thermal energy and mechanical energy, can be used as energy source for energy harvesters. Solar energy harvester [15, 16], thermoelectric energy harvester [17, 18], and piezoelectric energy harvester [19, 20] have been proposed based on these different energy conversion laws. Howerer, the widespread use of solar and thermoelectric energy harvesters is still limited by their complex structures and weather/temperature/place dependencies [21, 22]. Piezoelectric energy harvesters are more suitable for wearable electronic devices. One important reason is that the human body itself contains huge mechanical energy. Human lung movement, heart beat and blood flow can generate about 0.3-1W energy [23]. The movement of ankle, knee, hip, elbow and shoulder can generate several energy. These energy can be used by wearable piezoelectric energy harvesters to power variety of devices. In order to better fit with the human body to improve comfort, wearable energy harvesters need to have enough flexibility to withstand large tensile and torsional deformation, so they are also named flexible energy harvesters (FEHs). **Figure 2** shows representative applications of piezoelectric wearable or implantable energy harvesters and self-powered sensors [24-30]. These devices can be attached to the fingers, wrists, throats, feet and other positions for energy harvesting or movement monitoring.
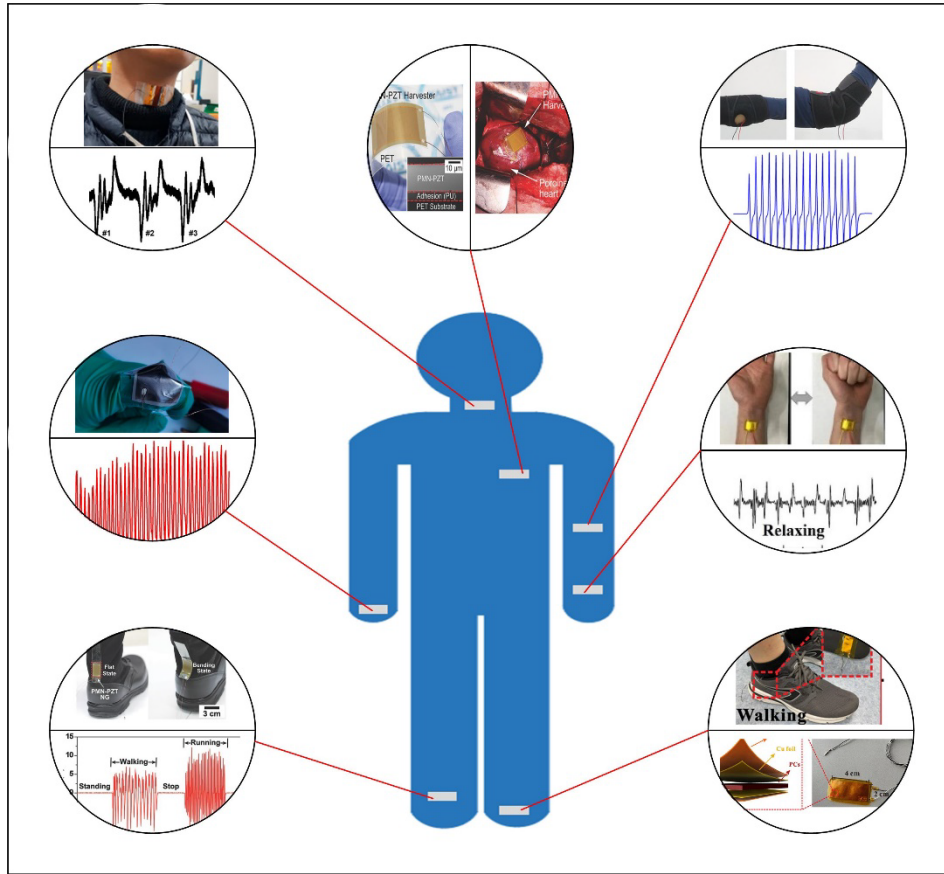
Figure 2. Application of piezoelectric wearable and implantable energy harvesters and self-powered sensor [24-30]

Piezoelectric materials can convert mechanical energy into electrical energy. They are sensitive to mechanical deformation and have high energy conversion efficiency. Morever, the wearable energy harvesters made of this material has simple structure and mature fabrication technology [31, 32]. For these reasons, wearable piezoelectric energy harvesters have been widely studied by researchers. Piezoelectric materials that can be used for energy harvesters include inorganic piezoelectric materials and organic piezoelectric materials. However, inorganic piezoelectric materials are usually brittle and unable to withstand large deformation, while organic piezoelectric materials has very limited energy conversion efficiency, which have hindered the their application in wearable energy harvesters. Therefore, piezoelectric composites composed of organic and inorganic materials have attracted the attention [33]. Since the 1950s, perovskite inorganic piezoelectric materials with ABO_3 structure have been regarded as a major breakthrough in the field of energy harvesting [34]. Various materials preparation methods have been developed for energy harvesters in recent years. Inorganic materials are mostly prepared by sputtering or liquid-phase synthesis method, while organic

piezoelectric materials and composites are ususally produced by casting, spin coating, electrospinning and 3D printing. At present, many reviews on piezoelectric energy harvesters have been published [35-39], but they usually involve a wide range of applications. There is a lack of a specific review about the wearable flexible piezoelectric energy harvesters. In recent years, with the rapid development of smart healthcare technologies, the novel wearable flexible piezoelectric energy harvesters have attracted extensive attention. As shown in **Figure 3**, the research output on wearable piezoelectric energy harvesters has been on an upward trend. Therefore, this paper aims to systematically summarize the research progress and achievements in this fast growing field. **Section 2** briefly summarizes the energy conversion principle of piezoelectric materials. Then, popular piezoelectric materials and their applications in wearable piezoelectric energy harvesters are discussed in detail in **Section 3**. Especially, the influence of piezoelectric phase characteristics (such as content, morphology, distribution and surface chemical modification) of piezoelectric composites on electrical energy output is analyzed and summarized. **Sections 4** and **5** present the novel structures and fabrication methods of current piezoelectric FEHs. Finally, the concluding remarks and future perspectives of wearable flexible piezoelectric energy harvesters are highlighted in **Section 6**.
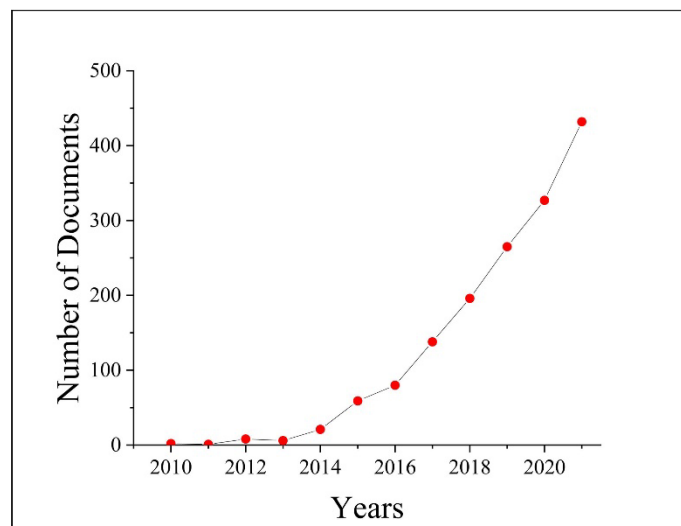

Figure 3. Number of documents on ("piezoelectric energy harvester" or nanogenerator) and (wearable) by year (data from Web of Science Core Collection)

2. Piezoelectricity

Piezoelectricity of materials is caused by their non centrosymmetric crystal structure. For all 32 crystal classes of materials, 20 of them exhibit piezoelectric properties [40]. When piezoelectric materials are deformed by mechanical stress, the positive and negative charge centers in the material will shift, resulting in charges generation on the surface, namely, piezoelectric effect [41]. Two separate electrodes are prepared on the surface of the piezoelectric material and connected to the external electric loading, allowing the free charge generated by piezoelectric materials flowing through the wire to power electronic devices. Perovskite structure and wurtzite structure materials are widely-used in FEHs. The perovskite structure can be expressed in the form of ABO_3. A and B represent a kind of cation respectively, or the mixture of two or more cations. The radius of A ion is close to that of oxygen ion, forming a dense stack. The radius of B ion is small, and it is located in the middle [42, 43]. The crystal structure of perovskite materials will change with temperature. Curie temperature is the phase transition temperature of piezoelectric materials from ferroelectric phase to paraelectric phase [44, 45]. When the ambient temperature is higher than the Curie temperature, the unit cell will be a cube, as shown in Figure 4 (a). The structure is centrosymmetric. When the external force is applied, the centers of positive and negative charge are still coincident, and the material shows no piezoelectricity. When the temperature drops below the Curie temperature, the unit cell will be a tetragon, as shown in Figure 4 (b). The structure is non centrosymmetric. When the external force is applied, the centers of positive and negative charges are separated, and the material has piezoelectricity. The wurtzite structure is a hexagonal crystal class. The reason for its piezoelectricity is that the non centrosymmetric crystal structure causes the separation of the positive and negative charge centers when it is pressed [40].
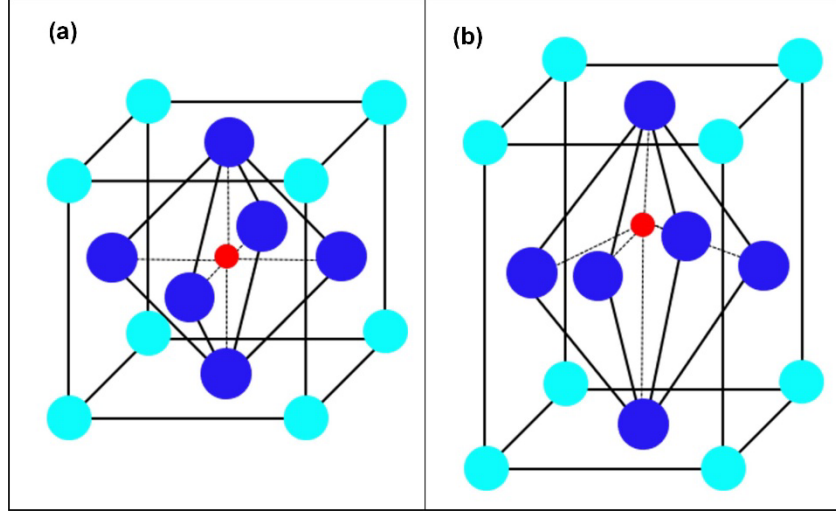
Figure 4. Unit cell of ABO3 material (a) cube unit cell; (b) tetragon unit cell

The properties of piezoelectric materials can be evaluated by different parameters, including permittivity (ε), dielectric loss factor (tan δ), elastic compliance constant (s), electromechanical coupling factor (k), Curie temperature (T_C) and piezoelectric constant [38, 42]. Their physical meanings are summarized in **Table 1**. Piezoelectric constant, including piezoelectric charge constant (d) and piezoelectric voltage constant (g), refers to the material conversion coefficients of mechanical energy and electrical energy. Piezoelectric materials are anisotropic, and the direction parallel to polarization axis is defined direction 3. Due to its anisotropy, piezoelectric constant could be expressed by a 3 × 6 matrix. Among them, d_{33} and represent the charge and the eletric field produced in direction 3 by an applied stress in direction 3, respectively. They are often used to evaluate the performance properties of energy harvesters. The piezoelectric voltage can be calculated by equations (1) and (2) [38]:

$$V_{OC} = \frac{d_{ij}}{\varepsilon_r \varepsilon_0} \sigma_{ij} g_e \tag{1}$$

or

$$V_{OC} = g_{ij} \sigma_{ij} g_e \tag{2}$$

where V_{oc} is open circuit voltage, σ_{ij} represents stress, d_{ij} and g_{ij} are piezoelectric charge constant and piezoelectric voltage constant, ε_r and ε_0 refer to the relative permittivity and vacuum permittivity, and g_e represents the distance between two electrodes. A large piezoelectric charge constant, a small permittivity or a large piezoelectric voltage constant are more favorable for achieving high voltage output.

10

Table 1. Evaluation parameters of piezoelectric materials

Category	Parameter	Description
Dielectric properties	Permittivity (ε), Relative permittivity (ε_r)	The ability of a material to store electrical potential energy
	Dielectric loss angle (δ), Dielectric loss factor (tan δ)	A dielectric material's inherent dissipation of electromagnetic energy
Elastic properties	Elastic compliance constant (s)	A parameter to describe the relationship between strain and stress
Piezoelectric properties	Electromechanical coupling factor (k)	A measure of the interchange of electrical and mechanical energy
	Curie temperature (T_C)	The temperature at which materials lose their ferro-magneticity and become paramagnetic
	Piezoelectric charge constant (d)	The polarization generated per unit of mechanical stress applied to a piezoelectric material
	Piezoelectric voltage constant (g)	The electric field generated by a piezoelectric material per unit of mechanical stress applied

3. Piezoelectric materials and its application in FEHs

In FEHs, the conversion from mechanical energy to electrical energy is realized by piezoelectric materials. Materials performance directly affects the performance of energy harvesters. To meet the requirements for power supply of electronic devices, piezoelectric materials are usually expected to have a strong energy conversion. Moreover, in order to maintain the good performance under the complex environment in human's body, materials should own some other excellent characterise, such as non-toxic, harmness, good impact and fatigue resistance which ensure the energy harvesters can work under alternating stress. At present, popular piezoelectric materials usually include inorganic piezoelectric materials, organic piezoelectric materials, and piezoelectric composites composed of piezoelectric ceramics and flexible matrix. **Figure 5** shows the piezoelectric materials that are widely used in FEHs.
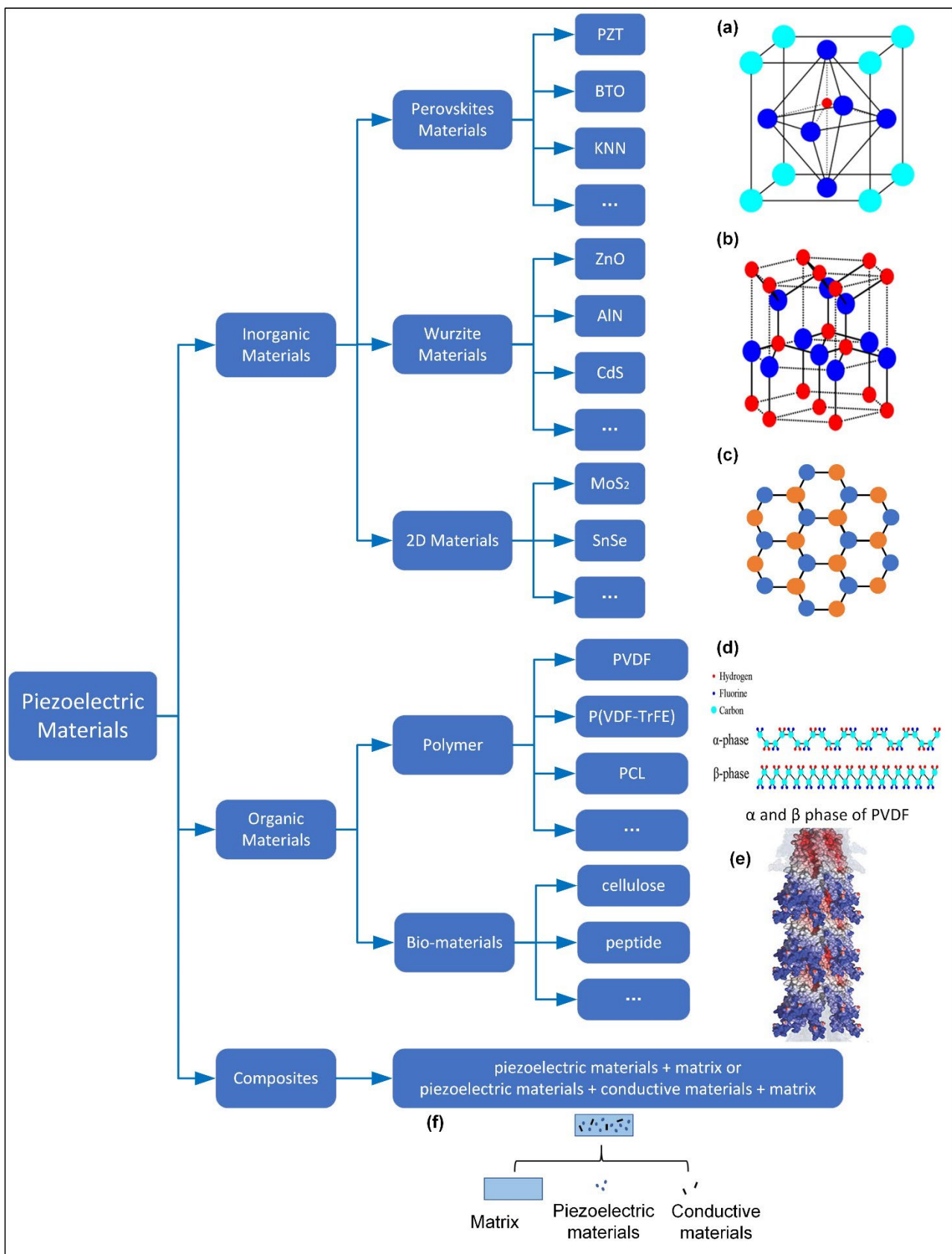
11

Figure 5. Popular materials for piezoelectric FEHs: (a) perovskite cell unit; (b) wurtzite cell unit; (c) structure of 2D materials such as MoS_2; (d) α-phase and β-phase conformations of PVDF; (e) Schematic of M13 phage with piezoelectric properties [119]; (f) Schematic of piezoelectric composites

12

3.1 Inorganic piezoelectric materials

Inorganic piezoelectric materials, such as perovskite ceramics, wurtzite materials and novel 2D piezoelectric materials, often have higher piezoelectric constants than organic piezoelectric materials, which means these materials exhibit good energy conversion performance. However, because of their brittleness, they are prone to fracture under long-term alternating stress, thus they are usually wrapped with flexible materials to form a 'sandwich' structure in practical application. Moreover, inorganic piezoelectric materials are usually prepared into nano or micron films in order to improve material ductility or produced into discontinuous forms (such as nanowire arrays, nanorod arrays, among others), which contributes to reducing stress concentration and improve their bearing capacity [46].

The crystal cell structure of perovskite ceramics is shown in Figure 4. Among them, lead-containing ceramic such as $Pb(Zr,Ti)O_3$ (PZT) has emerged as a hotspot due to its large piezoelectric constant [3]. However, since lead is toxic and harmful to human-body [22, 47, 48], lead-free piezoelectric materials have attracted extensive attention in wearable devices, including barium-containing ceramics, alkali niobate ceramics and bismuth-containing ceramics. Barium titanate ($BaTiO_3$, abbreviated as BT or BTO) is one of the earliest commercialized ceramics which have been widely used [49-51]. But they show a low Curie temperature and thermal stability [52]. Alkali niobate ceramics and bismuth-containing ceramics have much higher Curie temperature and high ferroelectric polarizability, which has attracted extensive attention [53-56].

Some piezoelectric ceramics are binary or multi-component materials, and the ratio of different elements and their preparation process have an impact on their performance. Shandilya and co-workers have conducted a lot of research on these materials, including $(Ba,Ca)TiO_3$ (BCT) [57] and $(K,Na)NbO_3$ (KNN or NKN) [58]. These studies provide an important reference for the selection of energy harvester materials.

The piezoelectric constant of these materials are shown in **Table 2** [3, 25, 29, 49-51, 53, 54, 59-67].

13

Table 2. Piezoelectric constants of widely-used perovskite piezoelectric ceramics.

Category	Materials	Piezoelectric constants d_{33} (pC/N)	Ref.
lead-containing ceramics	$Pb(Zr,Ti)O_3$	406	[3]
	$Pb(Mg_{1/3Nb2/3})O_3$-$PbTiO_3$	373±5	[59]
	$Pb(Mg_{1/3}Nb_{2/3})O_3-Pb(Zr,Ti)O_3$-Mn	1140	[25]
	$Pb(Mg_{1/3}Nb_{2/3})O_3$-$Pb(Zr,Ti)O_3$	1 527	[29]
barium-containing ceramics	$BaTiO_3$	105	[49]
	$BaTiO_3$	133 - 213	[50]
	$BaTiO_3$	206	[60]
	$BaTiO_3$	191	[61]
	$Ba(Zr_{0.2}Ti_{0.8})O_3$–$(Ba_{0.7}Ca_{0.3})TiO_3$	464	[51]
	$Ba(Zr_{0.2}Ti_{0.8})O_3$–$(Ba_{0.7}Ca_{0.3})TiO_3$	620	[62]
alkali niobate ceramics	$KNbO_3$	423	[63]
	$(K,Na)NbO_3$	50	[53]
	$(K,Na)NbO_3$	120	[64]
	$(K,Na)NbO_3$	182.5	[65]
bismuth-containing ceramics	$(Bi,Na)TiO_3$-$(Bi,K)TiO_3$	190	[54]
	$Na_{0.5}Bi_{0.5}TiO_3$-$K_{0.5}Bi_{0.5}TiO_3$-$BaTiO_3$	314	[66]
	$Bi_{0.5}(Na_{0.6}K_{0.4})_{0.5}TiO_3$	154	[67]

As the most widely-used wurtzite piezoelectric material, zinc oxide (ZnO) was applied in an energy harvester as early as 2006 [68]. ZnO is often prepared into discontinuous structures such as nanorods, nanowires and nanosheets to bear more stress and show a high energy conversion efficiency [39]. Kim *et al* [69] prepared ZnO nanorods with a diameter of 80 nm and a height of 2 μm for energy harvester by aqueous solution method. When a pressure of about 7.846 N was applied on the surface, the output current was 2.0 μA/cm^2. He *et al* [70] processed ZnO nanorods array with a diameter of 70 nm and a height of 2 - 3 μm. When the material is subjected to bending deformation, the open-circuit voltage and short-circuit current test were 2.8 mV and 8.5 mA. In addition, other wurtzite materials such as aluminum nitride (AlN) and cadmium sulfide (CdS) can also be used as piezoelectric materials for FEHs. For example, Algieri *et al* [71] sputtered AlN onto polyimide (PI) substrate to form a piezoelectric film, whose piezoelectric constant d_{33} is 4.93 ± 0.09 pC/N.

14

Under the excitation of bend loading, the output peak-to-peak voltage and current were 1.4 V and 1.6 µA. Zhang *et al* [72] prepared CdS nanosheets and magnetron sputtered nickel oxide on its top and bottom surfaces as electrodes of an energy harvester. After bending by fingertip, the peak-to-peak open-circuit voltage and short-circuit current were 1.2 V and 6 nA, respectively.

Wurtzite materials such as ZnO often shows weaker piezoelectric properties than perovskite materials. Although ZnO has obliged mankind with numerous applications such as thin film transistors [73, 74], gas sensors [75], biosensors [76], optoelectronic and photovoltaic devices [77, 78], it's usage in piezoelectric based devices is limited and efforts are going on to improve its piezoelectric response by doping it with various hetro-elements, including halogen dopants, transition metal dopants, rare earth metal dopants and others [40]. Batra *etl al* [79] prepared Tb-doped ZnO (Tb-ZnO) by wet-chemical co-precipitation method. After doping, the material morphology changed from hexagonal nanorods to nanotapers. Since the polarity of Tb–O bonds is higher than Zn–O bonds, the material is easy to be polarized, showing a higher piezoelectric property. Aleksandrova [80] successfully fabricated Ga-doped ZnO (Ga-ZnO), which also shows good piezoelectric properties. Under the action of a cyclic bending loading of equivalent 40 g, the energy harvester prepared with this material had an output voltage of 398 mV.

2D materials, such as graphene, MoS_2, because of their exciting physical, chemical, optoelectronic, and mechanical properties, are also used in flexible energy harvesters [81].Wu *et al* found [82] that voltage and current can be generated when cyclic stretching thin layer of MoS_2 with odd atoms. Research by Li *et al* [83] indicated that under bending excitation, 2D SnSe crystal they processed showed an output voltage of 760 mV and the power density 28 mW/m^2. In the work by Ghasemian *et al* [84], 2D piezoelectric materials are comprehensively reviewed from the aspects of preparation methods, piezoelectricity measurement approaches, and application. Currently, the application of 2D materials in FEHs is still rare, because of its relatively-low output energy, and the complexity and high cost of the preparation process. More exploration should be carried out to accelerate the creation of more 2D materials based FEHs.

The output voltages of representative FEHs made of inorganic piezoelectric materials are shown in **Figure 6** [3, 21, 29, 50, 53, 71, 72, 83, 85, 86].
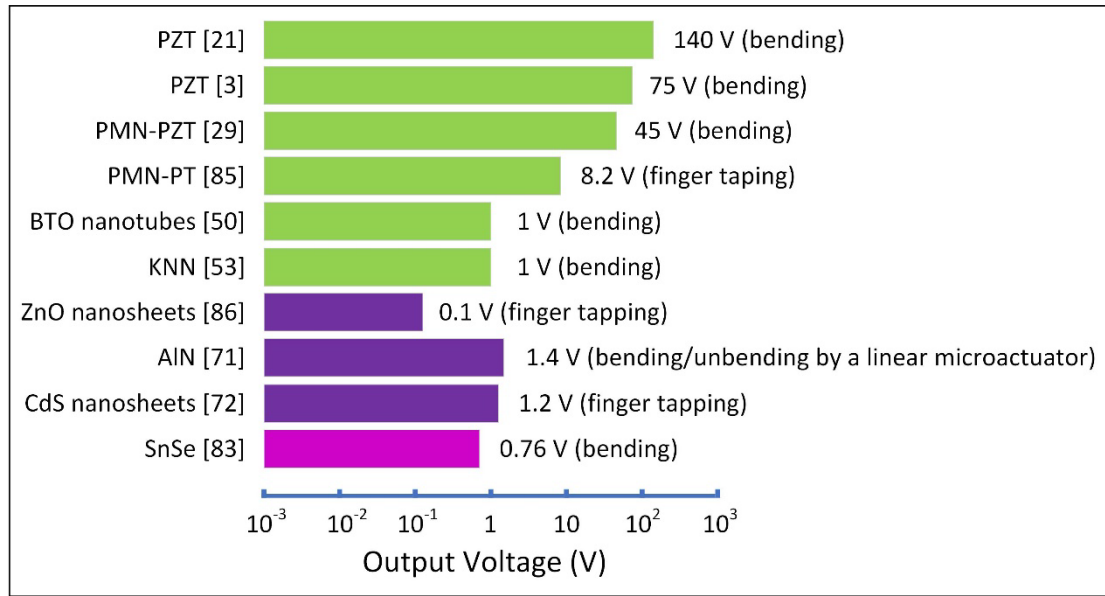
15

Figure 6. The output voltages of representative FEHs made of inorganic piezoelectric materials

3.2 Organic piezoelectric materials

Compared with inorganic piezoelectric materials, most of organic piezoelectric materials exhibit small piezoelectric constants, but they show great advantages in flexibility and lightweight [87, 88]. Moreover, they also have stable chemical properties, good biocompatibility and simple preparation process [89, 90]. Poly(vinylidenefluoride) (PVDF or PVF_2) and poly(vinylidenefluoride-co-trifluoroethylene) (P(VDF-TrFE)) are two popular piezoelectric polymers used in FEHs [90-92]. **Figure 7** compares the output voltages of several representative FEHs made of PVDF or P(VDF-TrFE) [90-95].
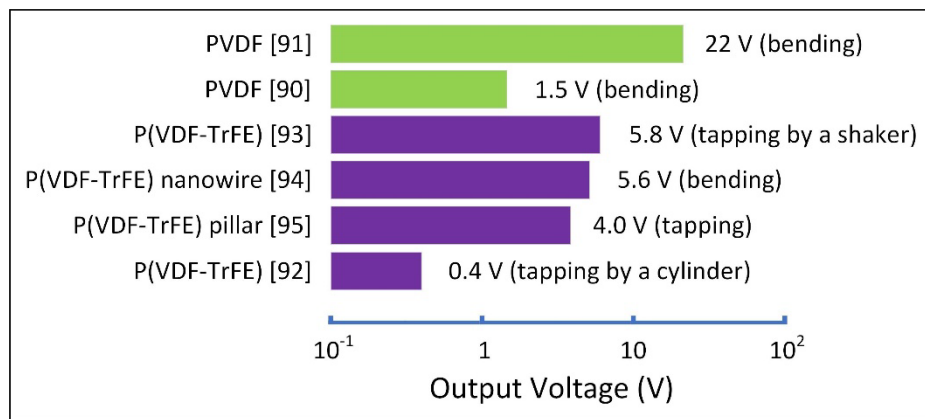

Figure 7. The output voltages of representative FEHs made of PVDF or P(VDF-TrFE)

PVDF   In 1969, Kawai discovered the piezoelectric properties of PVDF materials [96, 97], which has become the most widely-used piezoelectric polymer with piezoelectric constants d_{31} of 20 pC/N and d_{33} of 20

16

to 30 pC/N [91]. Despite of its small piezoelectric constants, the PVDF has a small permittivity, which leads to a high output voltage. PVDF shows different polymorphs, including α, β, γ, δ and ε. **Figure 5(d)** shows the conformations of most common phases, namely, α and β-phase [98]. α-PVDF is usually non-polar and does not have piezoelectricity, due to its random arrangement of hydrogen and fluorine dipoles, whereas β-PVDF exhibits good piezoelectric properties after its spontaneous polarization through electric dipole moments superimposition [99, 100]. Therefore, in order to improve the piezoelectric properties of PVDF, researchers improve the content of β-phase through various methods, including mechanical stretching [101-103], high-temperature annealing [104], external electric field polarizing [105], particles or reagents doping [106, 107].

Mechanical stretching is generally used to promote the transition from α-phase to β-phase by applying a mechanical stress in a reasonable direction to change the arrangement of polymer chains. During mechanical stretching, the conversion rate from α-phase to β-phase is affected by stretching temperature, ratio and speed. Mechanical stretching is usually carried out with high temperature annealing. Gomes *et al* [102] investigated the influence of stretching ratio and temperature (80-140 °C) on the performance of PVDF films. The testing results showed that when the temperature was 80 °C and the stretch ratio was 5, the content of β-phase in materials was the highest, achieving a large piezoelectric constant d_{33} of 34 pC/N. Li *et al* [103] studied the effect of stretching temperature (80-150 °C), speed (1 μm/s-1,000 μm/s), and ratios (1-5) on the performance of PVDF in terms of material microstructure and piezoelectricity. The PVDF showed the largest content of β-phase when temperature was about 100 °C and the drawing ratio was 3.

Electric field polarization also can be applied to change the direction of dipole moment, facilitating the transition from α-phase to β-phase. Ramos *et al* [108] found that when the applied vertical electric field exceeds 50 MV/cm, a rotation of –CF$_2$ and –CH$_2$ around the chain axis would happen in opposite directions. When the applied vertical electric field is larger than 100 MV/cm, α-phase would change into β-phase.

In addition, chemical particles, such as $Mg(NO_3)_2 \cdot 6H_2O$, Co_3O_4, can also be used as nucleating agents to promote and stabilize β-phase in PVDF, as indicated in the work by Chen *et al* [107] and Ojha *et al* [109].

P(VDF-TrFE)   P(VDF-TrFE) is produced by introducing trifluoroethylene (TrFE) into PVDF material, in which fluorine atoms will change steric hindrance, resulting in more β-phase in P(VDF-TrFE) [110].

17

Compared with PVDF, P(VDF-TrFE) has the advantages of high piezoelectric coefficient, good crystallinity, high residual polarizability and high temperature stability [93, 111]. Especially, good biocompatibility makes it applicable in wearable FEHs. The piezoelectric constant of P(VDF-TrFE) is between 20-40 pC/N [89, 112]. The methods to improve its piezoelectric properties include high-voltage polarization [92, 113], thermal annealing [114], nano particle doping [112] and so on.

Other piezoelectric ploymers   Some other polymers with piezoelectric properties are potentially applied in FEHs. For instance, poly(ε-caprolactone) (PCL) with good biocompatibility, has an orthorhombic crystalline structure unit with a space group $P2_12_12_1$, which is non centrosymmetric structure. Once PCL-based energy harvesters are subjected to external loading, the positive and negative charge centers of molecules will be separated and the charges will be generated on the surface. Using electrospinning, Sencadas [115] prepared PCL film with a polymer fiber size of 117 ± 17 nm, and the test piezoelectric charge constant d_{33} and piezoelectric voltage constant g_{33} were 5 ± 2 pC/N and 0.25 Vm/N. Zhu *et al* [116] used poly(l-lactic acid) (PLLA) as piezoelectric material to prepare nanofibers by electrospinning. When the bending deformation angle was 28.9°, the output open-circuit voltage and short-circuit current of the energy harvester could reach 0.55 V and 230 pA, and the joint movement-generated maximum power was 19.5 nW.

Piezoelectric bio-materials   Bio-materials such as collagen fiber, cellulose and chitin, also attracted the attention of scholars, due to their non-toxic and harmless, good biocompatibility, and easiness to synthesize [117-119]. Lee *et al* [117] found the piezoelectric behavior of M13 bacteriophage (phage). The piezoelectric constant of the phage self-assembled thin film was 7.8 pC/N, and the energy harvester could generate a current of 6 nA and a voltage of 400 mV. Ghosh and Mandal [120] extracted natural collagen nanofibers from the swim bladder as piezoelectric materials to make energy harvesters. The open-circuit voltage and short-circuit current generated by finger pressing were 10 V and 51 nA. However, biomaterials above-mentioned generally have low piezoelectric constants and the natural materials with high energy conversion ability need to be further developed.

For organic piezoelectric materials, PVDF and P(VDF-TrFE) are widely studied and applied, and mature technology ensures that such materials are still the research focus of piezoelectric organic harvesters. Other

18

piezoelectric polymers and natural materials are not widely used because of their low piezoelectric constants. The research and development of materials with high voltage electrical properties is a research hotspot for these materials.

3.3 Piezoelectric composites

Piezoelectric composites are composed of matrix and piezoelectric ceramics. The matrix absorbs stress and prevents material fracture, while ceramics realize energy conversion. Piezoelectric composites are expected to overcome the problems that inorganic piezoelectric materials are prone to failure under impact and fatigue loads, and piezoelectric organic materials have poor energy conversion effect.

The type of composite material can be defined by an index of two numbers, which correspond to the connectivity of ceramic and matrix material in three dimensions [121, 122]. The most studied piezoelectric composites are categorized into 4 types, namely, '0-3' type, '1-3' type, '2-2' type and '3-3' type, as shown in **Figiure 8**. '0-3' means that piezoelectric materials are dispersed in 3D-connected matrix, which is the most widely-used piezoelectric composite material for FEHs.
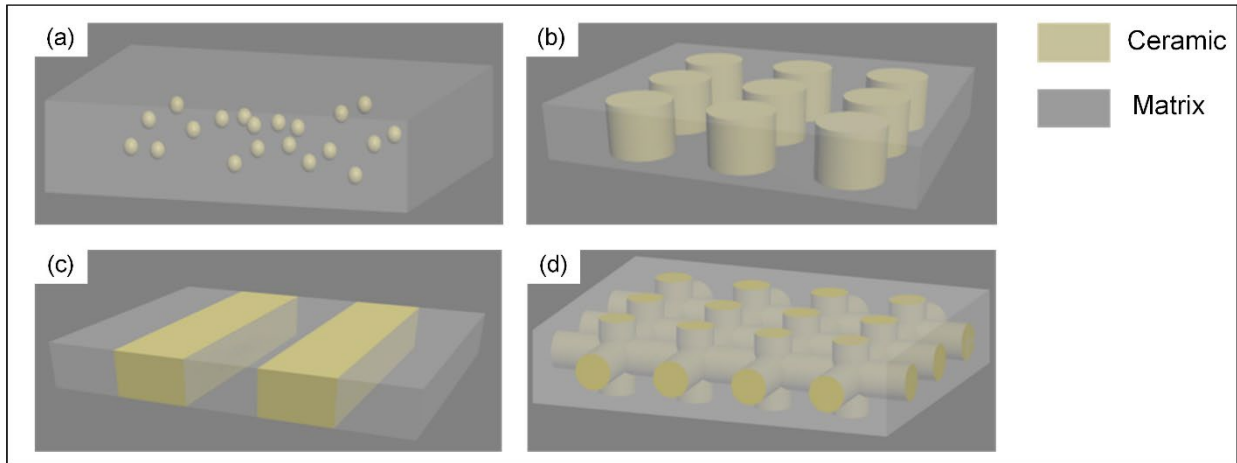

Figure 8. Schematic of widely-used piezoelectric composite structure: (a) '0-3'; (b) '1-3'; (c) '2-2'; (d) '1-3' type

3.3.1 Matrix

When external stress is applied on the piezoelectric composites, matrix will absorb the strain and affect stress transmission, which will further influence the energy conversion of energy harvesters [123]. The matrix also needs to be easy to process and non-toxic. Currently, the commonly-used matrix materials include

19

polydimethylsiloxane (PDMS) [124, 125], epoxy [126, 127], poly(methyl methacrylate) (PMMA) [128], polyurethane (PU) [22], polylactic acid (PLA) [129], polyether block amine (PEBA) [130], among others.

PDMS has been widely used in FEHs, due to its easy to access and storage, low cost, chemical stability, high elasticity and good biocompatibility [93, 123]. Its relative permittivity ε_r is about 4.6, which is smaller than that of PVDF (about 13) [131], based on the equation (1) in Section 2, composites with smaller permittivity can generate a larger output voltage. Zhuang et al [124] prepared KNN/PDMS composites with a piezoelectric constant d_{33} 6 pC/N. After being packaged into an energy harvester, the power generated by finger tapping was 0.13 μW. Shi and Beeby [132] fabricated ZnO/PDMS composite films by spin-coating. After polarization, the piezoelectric constant d_{33} was 380 pC/N. The peak value of output power was 0.78 μW when compressed with 150 N. However, the piezoelectric performance of ZnO/PDMS composite tend to weaken as time passed by. The piezoelectric constant reduced to 55% of the initial value after two weeks.

Piezoelectric polymers can also be used as matrix to protect internal piezoelectric ceramics because of their good flexibility. Piezoelectric polymer matrix also has piezoelectric behavior. High direct current (DC) voltage polarization of composites makes the direction of spontaneous polarization of piezoelectric ceramic and matrix consistent. Under the action of external stress, the electric field generated by the two materials will be synergy, making the output voltage higher [46, 133]. Pan et al [134] chose $Ba_{0.7}Sr_{0.3}TiO_3$ (BST) as ceramic phase and prepared BST/PVDF composite film by electrospinning. Under the alternating load, the output open-circuit voltage was 667 mV and the short-circuit current was 310 nA. Sahoo et al [135] fabricated the Fe-doped ZnO/P(VDF-TrFE) with the highest open-circuit voltage of 7 V when finger tapping. However, since piezoelectric polymers cannot directly dissolve ceramics, additional dissolving agent are needed in the prepraration process of composites. Both dissolution and solvent evaporation process will affect the final performance of the composites.

3.3.2 Piezoelectric phase

In piezoelectric composites, piezoelectric phase is mainly responsible for energy conversion. Its content, morphology, distribution and surface chemical modification will affect the performance of energy harvesters.

Content   Kim *et al* [136] added BTO particles of different mass fraction (0-15 wt%) to PVDF to form BTO/PVDF composites, which were further applied to prepared the piezoelectric film by fused deposition modelling (FDM) 3D printing, as shown in **Figure 9**. With the increase of BTO content, both number and size of ceramic aggregates in PVDF matrix increased. When the BTO content reached 9 wt%, microcracks were initially formed in the matrix, as shown in **Figure 9(d)**. As mass fraction increased, the cracks grew, leading to the decrease of the material strength. For piezoelectric performance, the output current would increase with the ceramic phase content. The current generated by composites with 15 wt% BTO was 0.0442 nA and the piezoelectric constant d_{33} was 0.101 pC/N.
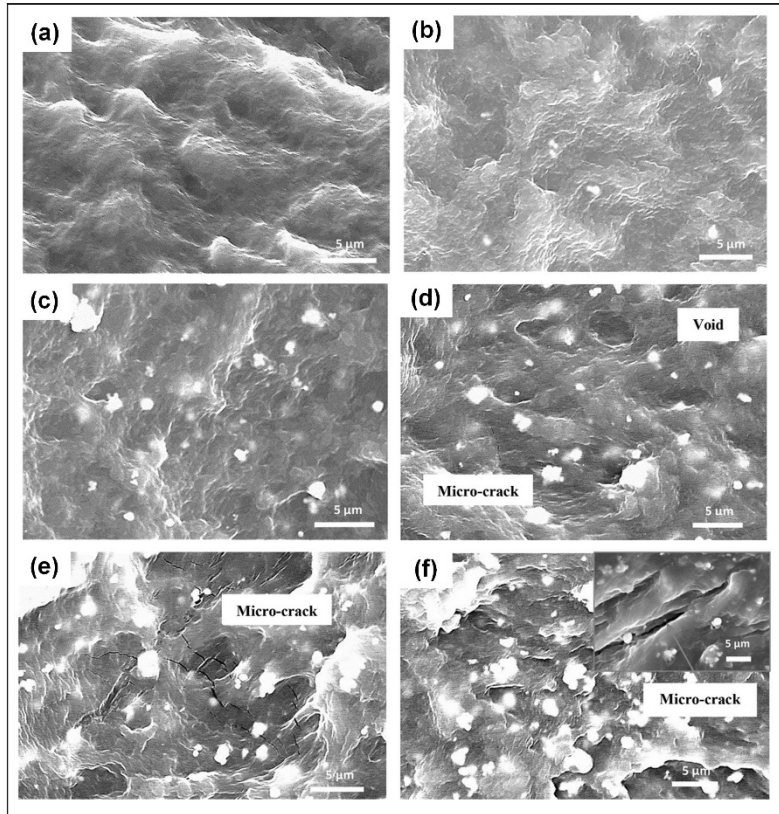

Figure 9. Composite film surfaces with different ceramic contents: (a) pure PVDF, (b)-(f) 3, 6, 9, 12, 15 wt% BTO/PVDF [136]

However, many research results show that the piezoelectric properties of the composites are not positively correlated with the ceramic content. Gaur *et al* [47] prepared BTO/PVDF composite films with different ceramic mass fractions (5-40 wt%), and measured the output voltage by finger tapping after polarization. The results show that the composite with 10 wt% BTO has the maximum output voltage of 78 V and power density of 120 $\mu W/cm^2$. With the further increase of ceramic content, the output voltage of the composite tend to

21

decrease. Many studies have drawn similar conclusions, but the accurate explanation of this phenomenon remains to be explored. Researchers give some explanations as follows [55, 65, 137, 138]: Firstly, the higher the content of ceramic phase, the more likely the cluster phenomenon caused by particle aggregation will occur, which will weaken the piezoelectric properties of the material; Secondly, the more ceramic phase content in the composite, the stress on each ceramic particle will be reduced, resulting in a low voltage output; Thirdly, the voltage output is related to the dielectric properties. The permittivity of the composite with high ceramic content is large, so the output voltage will be reduced. In addition, the appropriate ceramic content will facilitate the formation of β-phase in PVDF or P(VDF-TrFE) matrix materials. A very large content also easily leads to an increased amorphous polymer content and weakened piezoelectric properties.

Morphology　　In addition to ceramic particles, wires, rods, pillars, cube, platelets and even irregular flower-shaped ceramics can also be used as additive phase for piezoelectric composites.

Waseem *et al* [139] prepared GaN/Al$_2$O$_3$ nanowires with the length and diameter of 6.5 μm and 40 nm through vapor-liquid-solid growth technique, as shown in **Figure 10(a)**. After spin-coating PDMS on nanowires, electrodes were added and encapsulated to make energy harvesters. Under bending excitation, the maximum output voltage could reach 30 V. Bairagi and Ali [140] processed KNN nanorods/PVDF composite energy harvester, which has a maximum voltage of 3.4 V in finger tapping (about 1.1 kPa). Shin *et al* [141] fabricated Fe-doped BTO nanopillars/PDMS composite energy harvester. The nanopillars with diameter and height of 120 nm and 400 nm were prepared by mold patterning, as shown in **Figure 10(b)**. The peak values of the output open-circuit voltage and short-circuit current of FEHs are 10 V and 1.2 μA/cm^2 when 0.3 Mpa stress knocking. Allluri *et al* [142] prepared BTO nanocubes/PDMS composite with different mass fractions (5-25 wt%) by casting. **Figure 10(c)** shows the morphology of nanocubes in the composite. The FEHs with 15 wt% BTO show the largest output electrical signal under 988.2 Pa stress, whose peak-to-peak open-circuit voltage and short-circuit current were 126.3 V and 77.69 μA/cm^2. Gao *et al* [143] prepared BTO platelets and dispersed them on Indium-tin oxide (ITO) coated polyethylene terephthalate (PET). **Figure 10(d)** illustrates the preparation process of FEHs. The open-circuit voltage and short-circuit current generated by the FEH under bending were 6.5 V and 140 nA, respectively. Jian *et al* [138] designed and prepared flower-like BTO

22

piezoelectric fillers and mixed them with carbon nanotubes (CNTs) to fabricated BTO-CNT/PDMS composite, shown in **Figure 10(e)**. For the composite at a BTO content of 15%, under the compression loading of 50 N, the output open-circuit voltage and short-circuit current were 260 V and 50 μA. In addition, through COMSOL simulation, it is also found that stress concentration is easier to occur at the petals, and a large local stress may be the main reason for the significant enhancement of voltage output in the composites.

Nanofiber film can be prepared by electrospinning after mixing ceramic particles with polymers such as PVDF and P(VDF-TrFE), which is also widely-used to make energy harvesters [144, 145]. Siddiqui *et al* [146] dispersed BTO particles with a diameter of 100 nm in P(VDF-TrFE) and prepared piezoelectric nanofibers by electrospinning. The schematic of the energy harvester made of nanofibers and PDMS matrix and the topography of fibers are shown in **Figure 10(f)**. The maximum output open-circuit voltage and short-circuit current under the action of a compression force of 20 N were 12.46 V and 3.65 μA, respectively.
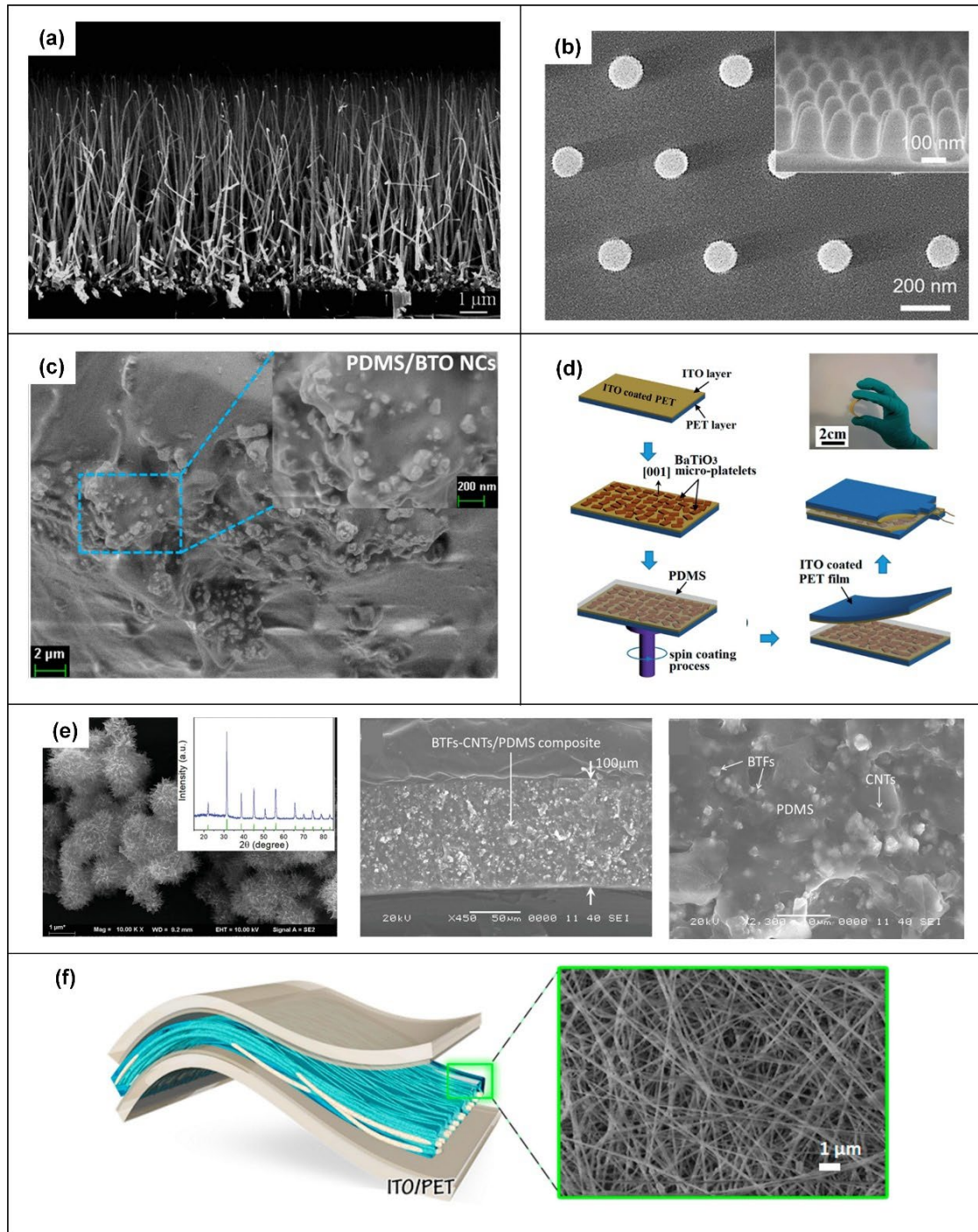
23

Figure 10. Piezoelectric composites with different ceramic morphology: (a) GaN/Al$_2$O$_3$ nanowires prepared by vapor-liquid-solid growth [139]; (b) Fe-doped BTO nanopillars array [141]; (c) BTO nanocubes/PDMS composite [142]; (d) Preparation process flow of BTO platelets/PDMS composite and photograph of FEH [143]; (e) Flower-like BTO and their dispersion in matrix [138]; (f) Schematic of BTO/P(VDF-TrFE) energy harvester made of nanofibers and PDMS matrix and SEM image of nanofibers [146]

24

From research results list above, we can know that the morphology of piezoelectric ceramic will affect the properties of materials. The stress distribution of the composite is different with the morphology of ceramic in the material. Generally speaking, stress is more likely to be concentrated on ceramics with morphology of wires, platelets and irregular flowers, which is conducive to the generation of electrical energy. However, ceramic stress concentration also increases the risk of material damage. The influence of ceramic phase morphology on piezoelectric properties of piezoelectric materials needs further research.

Distribution　　　The output electrical signals are also affected by distribution of piezoelectric phase. Once the distribution of ceramic particles in piezoelectric composites are well designed, the electric field generated by each ceramic particle can be superimposed. The practical distribution of phase distribution in composites is directly related to the materials preparation method.

Dielectric electrophoresis (DEP) is one of the widely-used methods to prepare piezoelectric composites with regularly distributed ceramics. By applying alternating current (AC) electric field during matrix curing, the ceramic particles are arranged regularly under the action of electric field force. Wang et al. [147] prepared aligned KN particles in PDMS matrix composite, shown in **Figure 11(a).** The experiment results showed that the electrical signals of the aligned composites were larger than those of randomly distributed piezoelectric particles composite. Gao *et al* [131] prepared $(Ba_{0.85}Ca_{0.15})(Ti_{0.90}Zr_{0.10})O_3$ (BCTZ)/PDMS composites by DEP. An AC electric field of 1 kV/mm and 50 Hz was applied during curing to ensure the ordered distribution of ceramics. Their research showed that under the action of the electric field, as curing time increased, the ceramic particles exhibited a more regular distribution. After polarization, the piezoelectric strain constant d_{33} and the piezoelectric voltage constant g_{33} were 31 pC/N and 600×10^{-3} Vm/N. The simulation results also showed that the ordered distribution ceramics contribute to better polarization of composites, resulting in a higher piezoelectric constants. Research by Hu *et al* [148] further verified this result. They prepared and compared the performance of piezoelectric composites with random and ordered distribution PZT nanowires and PDMS matrix, as shown in **Figure 11(b)**. They found that the open-circuit voltages of the energy harvester with random and orderly distribution of ceramics were 0.32 V and 0.6 V, and short-circuits were 2.44 nA and 3.95 nA.

Some other methods are also used to fabricate composites with regularly distributed ceramics. Gao *et al* [149] produced KNN nanowires/PDMS composites by extrusion 3D printing. During extrusion, nanowires adopted strongly preferential orientations in matrix due to the shear force in printing head. Test results showed that the maximum open-circuit voltage of printed composite was 72.2 V, which was about 400% of that of the materials with random distributed nanowires prepared by spin coating. Nafari and Scdano [150] also reached similar conclusions, confirming the superiority of well-ordered nanowire composites both theoretically and experimentally. Jin *et al* [151] studied the influence of an electric field on the distribution of $0.5Ba(Zr_{0.2}Ti_{0.8})O_3-0.5(Ba_{0.7}Ca_{0.3})TiO_3$ (BZT-BCT) nanofiber in composites. It was found that the applied electric field could help to realize the ordered distribution of nanofibers, as shown in **Figure 11(c)**. The output open-circuit voltage and short-circuit current of the nanofiber energy harvesters made of orderly-distributed nanofibers were 3 V and 50 nA, which are significantly higher than those (0.9 V and 12 nA) of energy harvesters with randomly distributed nanowires.
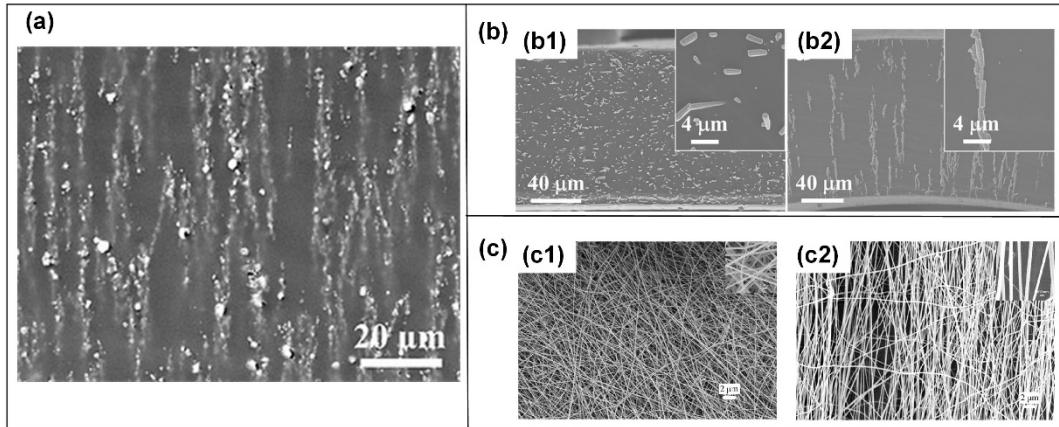

Figure 11. Piezoelectric composites with different ceramic distribution: (a) BCTZ/PDMS composite prepared by DEP [147]; (b) PZT nanowire composites with random distribution (b1) and ordered distribution (b2) [148]; (c) Randomly distributed BCTZ nanowires (c1) and regularly distributed BCTZ nanowires (c2) prepared by electrospinning [151]

Overall, although the orderly distribution of the ceramic phase inside the piezoelectric composites can help to improve the piezoelectric performance. The current preparation process cannot enable the controllable ceramic phase distribution. More work needs to be done for the optimization of the fabrication methods.

Surface chemical modification   As described above, the ordered distribution of ceramic particles in composites generally leads to a have higher output voltage. However, in the fabrication process, ceramic powders easily aggregate to clusters, reducing the mechanical strength and energy conversion performance [152]. Surface chemical modification of piezoelectric materials is an important method to reduce material cluster by coating organic components on the surface of piezoelectric particles to separate piezoelectric particles from each other. Surface modification of organic materials can also improve the bonding ability of ceramics and matrix, so as to facilitate effective stress transfer to piezoelcetric materials [153].

The surface modification of piezoelectric materials is achieved through chemical reaction. Ceramic particles are mixed with coating materials and organic solvents. After chemical reaction, surface modified piezoelectric ceramics can be separated from solvent by centrifugation. Gao *et al* [154] prepared 2-phosphonobutane-1,2,4-tricarboxylic acid (PBTCA) coated BTO nanoparticles by this method. BTO particles and PBTCA were mixed in alcohol solvent, stirred at 70 °C for 2h, cooled, centrifuged, washed and dried. They mixed PBTCA-coated BTO nanoparticles with P(VDF-TrFE) matrix to fabricate composite by casting. Under the vibration excitation, the maximum output voltage of the composite was 45 V and the current was 2.0 μA. Yang *et al* [155] used polydopamine (PDA) to modify the surface of BTO. After dispersing BTO into a buffer solution with pH 8.5, they added DA·HCl solution. Chemical reaction would happen to form PDA-coated BTO when strring solution. After centrifugation, cleaning and drying, particles were mixed with PVDF to fabricate energy harvester. Test results show that the energy harvesters with modificated materials exhibited a 2 times higher output than the untreated material. Guan *et al* [156] also used PDA as a modified coating to prepare a PTO/P(VDF-TrFE) self-powered sensor, whose output open-circuit voltage and short-circuit current were increased by 68% and 40% compared with the unmodified ones. In addition, gallic acid (GA) [157], PLA [158] are also used as modified materials , and good results have been achieved.

3.3.3 Conductive materials

For piezoelectric composites, the electric resistance of the matrix is very large. If conductive materials are added, the dielectric properties of the material can be changed. On the one hand, reducing the resistance of the matrix is conducive to the full polarization of the piezoelectric ceramics and improving the piezoelectric

constant [159]; On the other hand, the charge generated by piezoelectric ceramic is more easily transferred to the electrode, which has a better energy conversion performance.

Metallic materials such as silver and copper have low resistance and they can be used as conductive additives. Baek *et al* [160] added silver into BCTZ/PDMS composite, and piezoelectric constant d_{33} of the composite is about 220.5 ± 17.2 pC/N. Shin et al. [161] studied the influence of copper on the properties of BZT-BCT/PVDF material. The calculation results of COMSOL software showed that after adding copper particles, the composites would generate greater voltage under the same external force, which was also proved by their experiments.

Apart from conductive metals, carbon materials are also widely used in piezoelectric harvesters. In addition to their good conductivity, their unique physical and chemical properties have attracted much attention [162-164]. Such materials include multi-walled carbon nanotubes（MWCNTs）, graphene and carbon dots. MWCNTs have excellent conductivity, high specific surface area and high ductility [165]. In addition to improving the conductivity, it can also be used as a dispersant and stress enhancer. Park *et al* [166] processed BTO/PDMS composite with MWCNTs additives. Although the content of MWCNTs was very low, the output voltage and current were much larger than those of the composite without MWCNTs.

In addition to improving electrical conductivity, some materials such as graphene can also promote the formation of β-phase in piezoelectric polymer matrix of composites with piezoelectric polymer matrix. Anand *et al* [167] added graphene oxide (RGO) into the $Bi_2Al_4O_9$ nanorods/PVDF composites. The materials achieved a higher open-circuit voltage of 5.92 V than that of 3.19 V without the RGO composite under finger pressing with a pressure of 10 - 12 kPa. Wu *et al* [27] prepared the composite with PZT powder as piezoelectric materials, –OH-functionalized graphene (HOG) nanosheets as additives and P(VDF-TrFE) as matrix. They found that PZT and HOG can be used as nucleating agents to promote β-phase formation. However, excessive HOG nanosheets may lead to aggregation, which hindered the movement of P(VDF-TrFE) chains and inhibited the formation of β-phase.

In addition to the piezoelectric composite FEHs mentioned above, the output voltages of some other FEHs are summarized in **Figure 12.** [54, 123, 128, 142, 145, 156, 168-175].
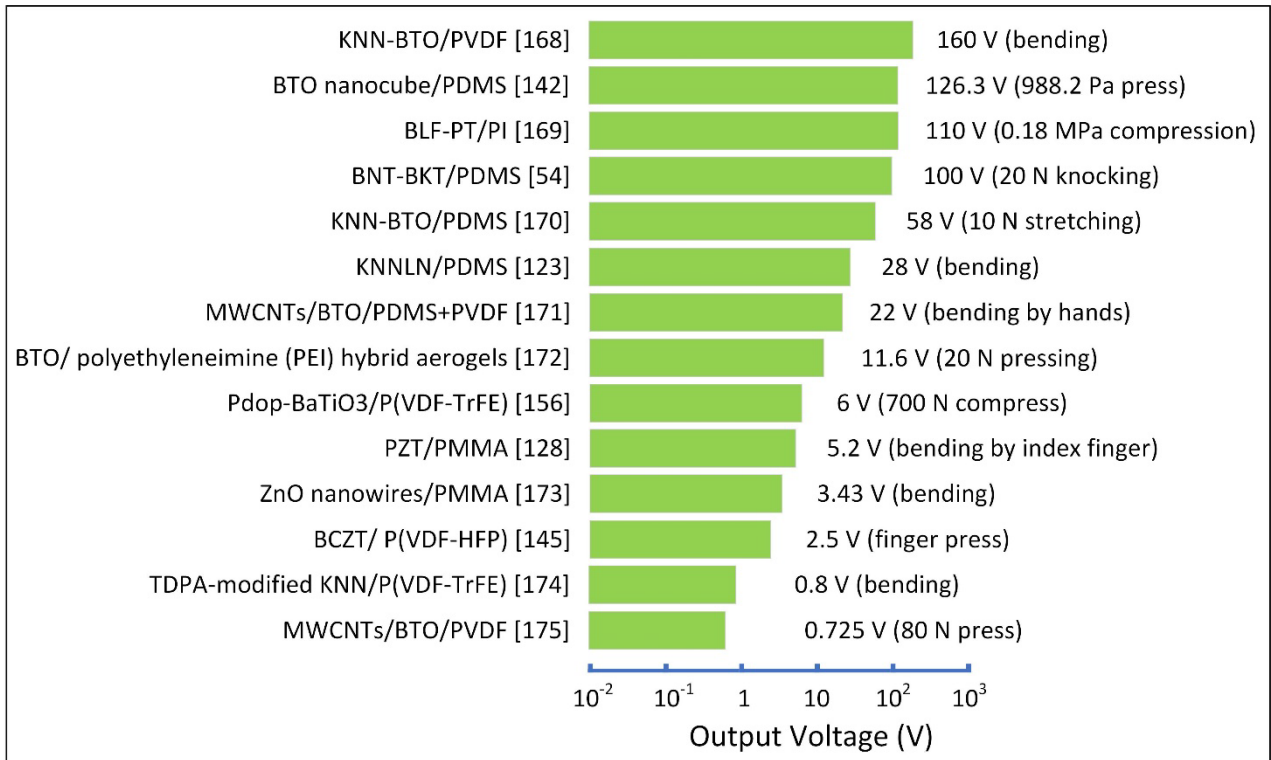
Figure 12. The output voltages of representative FEHs made piezoelectric composites

4. Novel structures of FEHs

The output electric energy of FEHs is related to its structure, which includes composite material structure and harvester shape. Types of composite material structure has been introduced in **Section 3.3**. The discussion above mainly involves '0-3' piezoelectric composites, which is the most widely-used type. In addition, '1-3', '2-2' and '3-3' type piezoelectric composites with better connectivity will be introduced in this section.

Chen *et al* [176] designed an energy harvester with self-connected piezoelectric P(VDF-TrFE) fiber array, whose structure is similar to '1-3' composite. The preparation principle and process is shown in **Figure 13(a)**. Under the force of 50 N and frequency 1 Hz, the energy harvester had a peak output voltage and current destiny of 13.2 V and 0.33 $\mu A/cm^2$. In addition, they also used electrohydrodynamic (EHD) method to prepare energy harvesters with similar structure, whose output voltage and current were 5.6 V and 2.6 μA under 25 N force [95]. The composites of '2-2' and '3-3' type have a better connectivity, which means a better mechanical transmission effect on ceramics phase [177]. Zeng *et al* [178] developed a '2-2' piezoelectric composite by cutting, grinding and polishing. The piezoelectric component was $Pb(In_{1/2} Nb_{1/2})O_3-Pb(Mg_{1/3}Nb_{2/3})O_3-PbTiO_3$ (PIN-PMN-PT) crystal, and the matrix was epoxy. The open-circuit voltage and current output of

29

FHEs under bending load were 54.2 V and 6.7 µA. Hao *et al* [179] prepared a '2-2' type composite energy harvester with $0.2Pb(Zn_{1/3}Nb_{2/3})O_3-0.8Pb(Zr_{1/2}Ti_{1/2})O_3$ (PZN-PZT) interconnecting skeletons by freeze-drying method. Experiment results showed that energy harvesters with this structure have ultra-high piezoelectric properties, and the calculated transduction coefficient $d_{33} \times g_{33}$ is 58 213×10^{-15} m²/N. Zhang *et al* [180] also prepared the FEH of $Pb(Mg_{1/3}Nb_{2/3})O_3-PbTiO_3$ (PMN-PT) material with cellulose skeleton through a similar method. The preparation process is shown in **Figure 13(b)**. Under the compression of 35 N, the output open-circuit voltage and short-circuit current were 36 V and 850 nA/cm², which is 4 times than that without cellulose template.

A reasonable shape can improve the electrical output of FEHs effectively. The shape design of energy harvesters has gradually attracted the scholars' attention. Wang *et al* [181] designed an energy harvester with 3D grid architecture shown in **Figure 13(c)**, which was prepared by extrusion 3D printing. The silver-coated $Pb(Ni_{1/3}Nb_{2/3})O_3-PbZrO_3-PbTiO_3$ (PNN-PZT) powder was mixed with PDMS, and then encapsulated after extrusion. The piezoelectric voltage constant g_{33} measured was 0.4 mV/N. The generated energy could instantly light up 20 commercial Light Emitting Diode (LED) lights under 20 N impact.

In addition, the practical working scenario of wearable energy harvesters was also considered in the design process. Human's skin strain can reach 30% during body movement, which is unachievable for traditional energy harvesters [182]. Therefore, Zhou *et al* [183] designed energy harvesters with kirigami structure, shown in **Figure 13(d)**. When their energy harvester subjected to stress, the shape can be easily adjusted with the skin, which will be more comfortable to wear. Experiment result showed that this kirigami structure could be stretched to more than 300% of its original shape, showing great potential for application in wearable electronic systems.
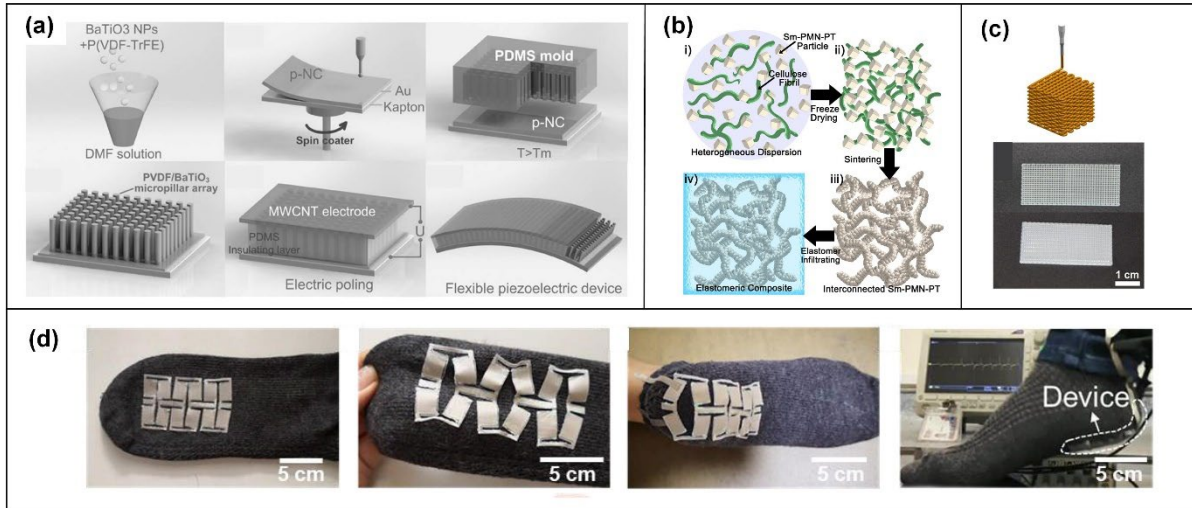
30

Fiugre 13. Schematic of FEHs with different structures: (a) Preparation process of self-connected piezoelectric P(VDF/TrFE) fiber array [176] ; (b) Schematics of the fabrication for the 3D interconnected porous piezoceramic skeleton based on cellulose template [180]; (c) 3D grid architecture energy harvester [181]; (d) Optical images of origami structure energy harvester mounted on a sock [183]

5. Fabrication methods

In recent years, preparation methods of FEHs have been improved and developed constantly. This section mainly discusses the preparation methods of popular inorganic piezoelectric materials, organic piezoelectric materials and piezoelectric composites.

5.1 Fabrication methods for inorganic piezoelectric materials

5.1.1 Sputtering and deposition

Sputtering and deposition methods are usually used to to fabricate the films by accelerating ceramic particles and impacting them on the substrate. Based on different particle formation and acceleration principles, sputtering and deposition methods for the preparation of piezoelectric energy harvesters can be divided into a variety of types including radio frequency (RF) sputtering, pulsed-laser deposition, aerosol deposition and so forth.

RF sputtering   RF sputtering is generally carried out in a near-vacuum environment. Positive ions in the RF discharge plasma are used to bombard the target, and the sputtered material is deposited on the substrate, thereby forming the film. RF voltage and post heat treatment temperature have influence on the fabricated

film. Aleksandrova *et al* [184] prepared ZnO/Ga$_2$O$_3$ films at different voltages of 0.5 kV, 0.9 kV and 1.1 kV. The SEM image of the prepared film is shown in **Figure 14(a)**. When the voltage increased to 1.1 kV, a large number of materials were sputtered onto the substrate, which provides more locations for grain growth to achieve a smaller grain size, and decreased the surface roughness, resulting in better piezoelectric properties. In the work by Kim *et al* [53], KNN films with a thickness of 45 nm were prepared on a titanium nitride-silicon substrate by RF sputtering, and they were treated at different temperatures (room temperature, 100, 200, and 300 °C). When the heat treatment temperature was lower than 200 °C, smooth piezoelectric film surfaces could be obtained with a small surface roughness, and the main composition was amorphous KNN. Under the bending excitation, the open-circuit voltage of the energy harvesters was less than 0.5 V and the short-circuit current was less than 20 nA. When the heat treatment temperature reached 300 °C, the surface roughness increased and KNN began to crystallize. The crystalline material showed better energy conversion effect. The open-circuit voltage was 1 V, and the short-circuit current was 30 nA. Aleksandrova *et al* [63] sputtered KNbO$_3$ (KN) on a flexible polyethylene naphthalate (PEN) substrate. Due to the limited heat resistance of PEN, a low temperature environment (110 °C) was chosen. At a sputtering voltage of 0.6 kV to 0.9 kV, the achievable thickness of prepared film was 265 nm-370 nm. SEM images showed that at a small sputtering voltage, irregular clusters would be formed on the substrate due to insufficient energy. As the voltage increased, the film become more uniform. When the voltage reached 0.9 kV, the KN film showed the finest and most regular microstructure.

Pulsed-laser deposition   To fabricate a film by pulsed-laser deposition, the target is bombarded by laser, and the sputtered material is deposited on the substrate. The deposition resolution and efficiency are higher than that of RF sputtering. Kang *et al* [185] first sputtered KNN on the substrate, and the KNN nanowire array was obtained by crystal growth. The following optimal process parameters were determined through experiments: the substrate temperature, laser energy, repetition rate, and number of laser pulses were 700 °C, 1.6 J/cm^2, 10 Hz and 18,000 times, respectively. The prepared nanowires have a diameter of 60 – 90 nm and a length between 500 – 600 nm, as shown in **Figure 14(b)**. The piezoelectric constant d_{33} of the nanowires is 97 ± 11 pC/N, which is higher than that of the film 48 ± 5 pC/N.

Aerosol deposition Aerosol deposition (AD) can be used to prepare large thickness piezoelectric films. The micron-sized piezoelectric particles are accelerated to about 300 m/s and then collide with the substrate at a high speed, thereby forming a dense ceramic film on the substrate. After AD, annealing treatment is usually required to promote grain growth and film crystallization, thereby improving piezoelectric performance. In the work by Hwang *et al* [3], the PZT particles were preheated at 400 °C, and then they were carried by medical grade dried air to collided with the sapphire substrate in the vacuum chamber, forming a piezoelectric film on the substrate surface. Subsequently, high-temperature annealing was performed to promote the crystallization of PZT. The grain sizes of the ceramics formed at annealing temperatures of 700 °C, 800 °C and 900 °C were 61.6 nm, 84.5 nm and 125.4 nm. With the increase of annealing temperature, the crystallization effect also became better. But when the temperature was higher than 900 °C, PbO will be evaporated, weakening the piezoelectric properties of the PZT. Under finger bending, the open-circuit voltage and short-circuit current of the piezoelectric film prepared at 900 °C were 200 V and 35 μA, which was 7.5 times of that of the film prepared at 700 °C.

5.1.2 Liquid-phase synthesis

Liquid-phase synthesis, as one preparation method of piezoelectric material in solution, is more economical than deposition methods requiring sophisticated equipment. Currently, the liquid-phase synthesis methods that can be used for the fabrication of piezoelectric energy harvesters including sol-gel method, hydrothermal method, among others.

Sol-gel method The precursor solution is poured or spin-coated on the substrate, and a specific temperature is set to volatilize organic components in the precursor to obtain the piezoelectric film. Jeong *et al* [21] prepared a PZT ceramic film with a thickness of 2 μm on a sapphire substrate by this method. The PZT sol-gel solution was spin-casted at 2500 rpm followed by pyrolysis in air environment at 450 °C for 10 min to form the film. After that, the film was transferred to a flexible substrate by laser lift-off technology. The encapsulated energy harvesters could generate a voltage of 140 V and a current of 10 μA under the bending of the finger.

33

Hydrothermal method   Hydrothermal method is used to prepare piezoelectric materials through hydrothermal reaction under high pressure, and it does not require a high temperature required for this process is not high (generally less than 200 °C) [186]. Manjula *et al* [86] synthesized ZnO nanosheets networks by a single-step hydrothermal method. The cleaned aluminum plate was placed in a solution of Zinc nitrate hexadehydrate ($Zn(NO_3)_2 \cdot 6H_2O$) and hexamethylenetetramine, and reacted in a hot air oven at a temperature of 80°C for about 4 hours. The ZnO obtained after cleaning and drying is shown in **Figure 14(c)**. The open-circuit voltage of energy harvesters generated by a finger tapping was 100 - 150 mV.

Hydrothermal method can also be used to prepare ceramic phase in piezoelectric composites. Wang et al. [171] fabricated BTO nanowires by hydrothermal method. Firstly, the Ti foil substrate was oxidized at 750 °C for 8 hours, then the oxidized substrate was introduced into a Teflon-lined autoclave filled with NaOH solution and reacted in an oven at 210 °C for 8 hours to obtain sodium titanate nanowires arrays. After soaking them in an autoclave of barium hydroxide octahydrate ($Ba(OH)_2 \cdot 8H_2O$) solution and reacted in an oven at 210 °C for 12 hours, BTO nanowire arrays with a wire width of about 330 nm could be obtained. Using this material and MWCNTs, a composite energy harvester based on PVDF matrix was prepared and 22 V voltage can be generated by finger bending.

Jeong *et al* [50] combined the hydrothermal method with the anodic oxidation method to prepare the array of BTO nanotube piezoelectric materials, and the process is shown in **Figure 14(d)**. First, the cleaned Ti foil was connected to the electrode and placed in an electrolyte solution. 60 V voltage was applied for anodic oxidation. During oxidation, the volume of the Ti substrate would expand, resulting in irregular surface and forming TiO_2 nanotubular. After reacting with $Ba(OH)_2 \cdot 8H_2O$ solution at 150 °C for 4 hours, BTO nanotubes could be synthesized. The piezoelectric constant d_{33} of the prepared material was 180.3 pC/N.
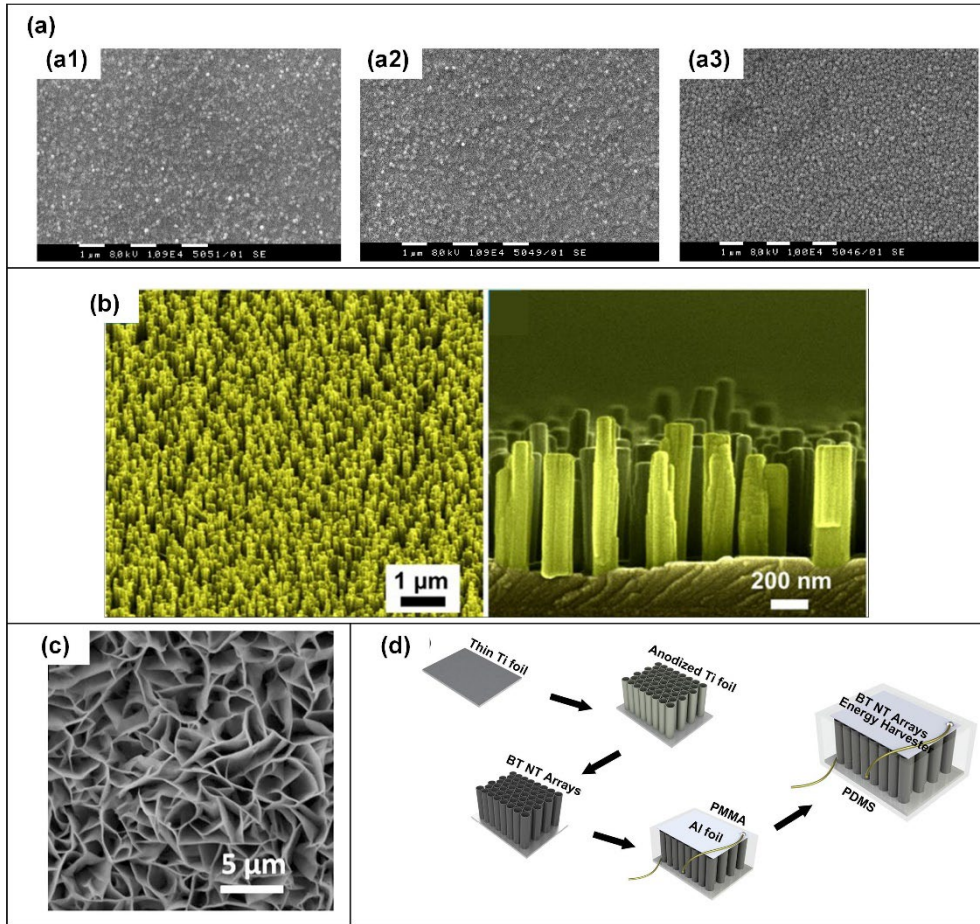
Figure 14. Preparation methods of inorganic piezoelectric materials: (a) Morphology of ZnO/Ga$_2$O$_3$ films sputtered at different voltages ((a1) 0.5 kV, (a2) 0.9 kV and (a3) 1.1kV) [184]; (b) KNN nanowire arrays prepared by pulsed-laser deposition [185]; (c) ZnO nanosheets networks synthesized by hydrothermal method [86]; (d) Preparing process of nanotubes by anodic oxidation [50]

5.2 Fabrication methods for organic piezoelectric materials and piezoelectric composites

The preparation methods of organic piezoelectric materials and piezoelectric composites are similar, which are introduced in detail in this section:

Casting   Casting is one of the simplest fabrication methods. Firstly, the solution containing piezoelectric components is poured into the Petri dish or other molds, and then the piezoelectric film can be prepared by chemical reaction, evaporation of solvent or curing in high temperature environment. Annealing treatment is always required in order to improve the performance of high voltage films. Vivekananthan *et al* [168] fabricated the KNN-BTO/PVDF composite energy harvester by casting. First, ceramic particles and the matrix were mixed and sonicated for 1 h by a probe sonicator. After that the solution was poured into glass Petri dish

35

and dried at 70 °C to form a composite film. The energy harvester was made up via the direct attachment of electrodes. Under the applied force of 0.4 N, the output open-circuit voltage and short-circuit current were 160 V and 400 nA. Casting process is easy, but requires a long curing time. Due to the different properties of each component in the solution, the materials will precipitate, and the high-density components are easy to accumulate at the bottom, making the film composition uneven.

Spin-coating　　　Spin coating is a procedure used to deposit thin films onto substrates. Material solution is gradually droppe on the continuously rotating substrate, spread under the action of centrifugal force, and cured through heat treatment and/or other processes to form a film. Jin *et al* [187] prepared Li-doped ZnO/P(VDF-TrFE) composites by spin-coating at the rotation speed 1,500 rpm. The film was obtained after it was dried in an oven at 50 °C. After annealing at 135 °C for 2 h and polarization in a 50 MV/m electrical field at a 100 °C for 1 h, the peak-to-peak output voltage of the prepared energy harvester was 3.43 V. This method can form the film layer by layer, which avoids long-term settling and ensures that each layer is uniform. However, it is necessary to select the appropriate rotation speed during spin-coating, the speed affects the centrifugal force, and the unreasonable centrifugal force will affect the processing result. Spin-coating is suitable for preparation of thin film. For thick films, multiple spin-coating should be done, resulting in low efficiency and unfavorable industrial production [188].

Electrospinning　　　Under the action of electric force, materials in the needle are ejected and deposited on the rotating drum collector to form nanofibers. The schematic structure of the electrospinning process is shown in Figure 15(a) [189]. During process, some parameters, which affect the forming performance and the formation of the β-phase of PVDF materials, should be considered carefully, including solvent properties, ejected speed, ambient temperature and humidity, nozzle shape and size [190]. Szewcyk *et al* [191] fabricated PVDF films by electrospinning. The preparation process parameters were: voltage 15 kV, nozzle inner diameter 0.8 mm, flow rate 6 mL/h, spinning time 8 min, and ambient temperature 25 °C. Two humidity, 30% and 60% were selected. The results showed that the content of the β-phase of film prepared at 60% humidity was twice that of 30%, and the piezoelectric constant d_{33} (5.558 pC/N) of the material is also higher. The fibers prepared by electrospinning are staggered with high flexibility. The application of high-voltage electric

36

field during processing is beneficial to the formation of β-phase, improving the piezoelectric properties of PVDF-based materials. However, process parameters should be controlled strictly to avoid failure preparation.

3D printing   3D printing, also known as additive manufacturing, can be used to fabricate parts or objects by layer-by-layer material accumulation, which provides a huge opportunity for the rapid preparation of electronic devices with complex structures [192].

Park *et al* [130] printed a BTO/PEBA piezoelectric energy harvester with nanocomposite deposition system (NCDS). The printed process parameters were: extrusion pressure 50 kPa, nozzle diameter 500 μm and printing temperature 150 ℃. Under compressive force, the average open-circuit voltage and short-circuit current were 2 V and 50 nA. Kim *et al* [193]compared BTO/PVDF piezoelectric films prepared by FDM 3D printing and casting. During 3D printing, the printing head temperature was 220 ℃ and the printing speed was 5 mm/s. Surface morphologies are shown in **Figure15(b)**. A large BTO agglomerate can be found on the bottom surface of casting film and more cracks were generated, while there was an obvious improvement in 3D printed film. This is because 3D printing-based materials can be formed and cured layer-by-layer, thereby avoiding the sedimentation during the curing.

In the above-described piezoelectric composites, horizontally-distributed nanowires composites can be prepared by extrusion 3D printing. **Figure 15(c)** shows the schematic of extrusion printing and the stress distribution in the printing needle. The flow velocity gradient of material at the edge of the cylindrical print nozzle is large, leading to a large shear force. The nanowires are forced to rotate and eventually distribute along the axial direction [129]. Malakooti used this method to process BTO/PLA energy harvesters with horizontally-distributed nanowires. After transferring configured ink into needle with the diameter 400 μm, printing has been carried out through a high-precision three-axis moving platform. The adjustment of printing pressure and speed is realized by G code. When the energy harvester was stretched with a strain of 0.35%, the root-mean-square value of voltage V_{RMS} and peak-to-peak voltage V_{PP} were 486 mV and 1.4 V, and the generated maximum power is more than 700% of that prepared by casting.

In addition, 3D printing can also be used for the preparation of complex structures. The fabrication of grid architecture energy harvester shown in **Figure 13(c)** is difficult to fabricate by traditional methods. But it can

be realised through extrusion 3D printing which is based on three-axis platform moving and materials distributing [181]. The kirigami energy harvester shown in **Figure 13(d)** can also be realized by 3D printing. The inner diameter of the nozzle used was 0.26 mm, and the printing speed was 10 mm/s. After printing, the solvent was evaporated rapidly in the environment of 70 °C to obtain the designed kirigami structure [183]. The advantages of these structures have been introduced in **Section 4**.

To sum up, in the preparation of energy harvesters, 3D printing technology mainly has the following advantages: (1) Layer-by-layer forming and curing results in a more uniform distribution of components in the composite; (2) Composites with ordered distribution of nanowires can be prepared by controlling the shear force during extrusion; (3) Through materials distribution on demand, energy harvesters with complex shape and structure can be prepared easily. However, the current research on 3D printing of piezoelectric materials is still in its infancy, and more materials suitable for 3D printing still need to be explored, as well as the design of printing processes and complex structures.
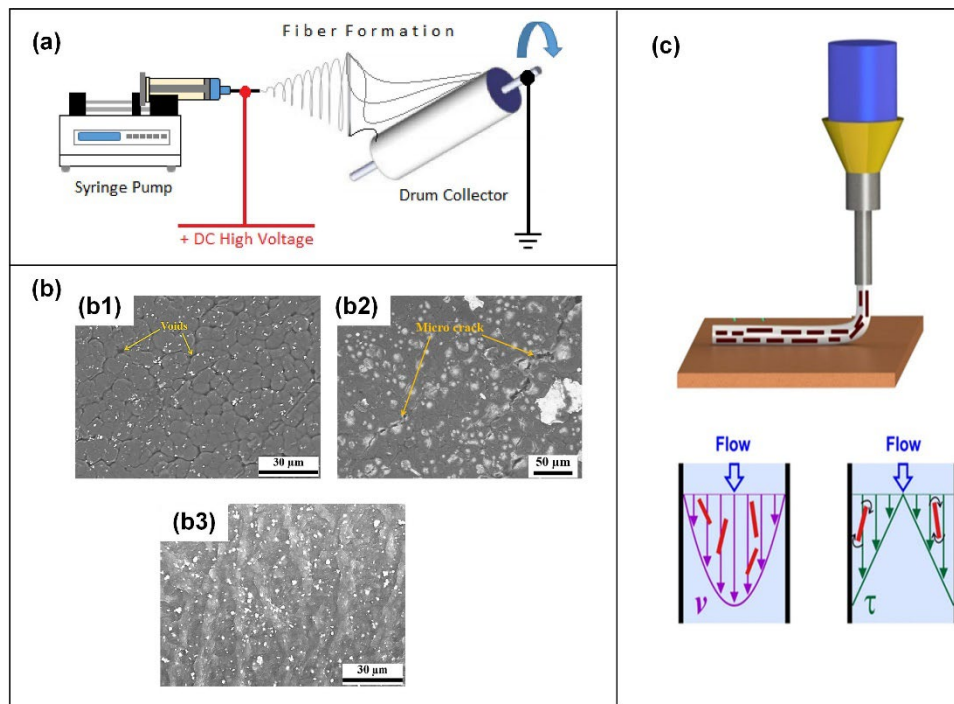

Figure 15. Preparation methods of organic piezoelectric materials and piezoelectric composites: (a) Schematic of electrospinning process [189]; (b) SEM images of composite surface ((b1) and (b2) top and bottom surfaces of solvent-casted film, (b3) surface of 3D printed film) [193]; (c) Schematic of extrusion printing and the stress of distribution in the printing needle [129]

38

6. Conclusions and outlook

Mechanical energy generated within human movement has demonstrated hugh potential in enabling the power supply of the wearable electronic devices through wearable piezoelectric flexible energy harvesters. In this review, we summarize the recent progress and achievements of wearable piezoelectric FEHs in terms of material, structure and fabrication. The principle of piezoelectric FEHs is first introduced. Then we review the frequently-used piezoelectic materials in FEHs, including inorganic piezoelectric material, organic piezoelectric material and piezoelectric. Additionally, the research finding on the influence of the content, morphology, distribution and surface chemical modification of ceramic phase in piezoelectric composites on piezoelectric properties are analyzed. Finally, the novel structures and fabrication methods of FEHs are discussed. On this basis, the results and the prospects for future research are drawn as follows:

(1) High energy output is the purpose of design and development of novel FEHs. Piezoelectric composite usually adopts a much more simply preparation process than inorganic materials and can withstand more impact and alternating loads, showing a high potential in novel FEHs, but the influence of the content, morphology and distribution of ceramics and conductive materials on the energy output remains unclear and needs further research;

(2) Traditional preparation methods such as spin-coating, RF sputtering, electrospinning are only applicable to produce simple structures. 3D printing shows a huge poential in fabricating complex structure because this method realise the fabrication of complex composites by means of point-by-point into line, line-by-line into plane, and plane-by-plane into a 3D part. This technology is still in its fancy. Further attention should be paid on 3D printing of piezoelectric composites with controllable shape and performance;

(3) At present, a lack of general performance test and evaluation method for energy harvesters has become one key bottlenck. Different excitation, mechanical force and frequency are used for FEH performance test, making it diffcult to compare results directly. In addition, most studies only consider the energy conversion performance but ignore the mechanical properties of the energy harvesters. FEHs are usually subjected to alternating loads, the effect of which on the service life and output of FEHs requires further investigation;

39

(4) 'Sandwich' structure is widely-used in wearable FEHs, but it ignores the influence of practical application conditions and scenarios (for example, when the FEHs are attached to an elbow or a sock). Innovative design, miniaturization, integration, intelligence and personalized design should be considered in the research and creation of future FEHs.

In conclusion, the design of flexible piezoelectric energy harvesters is still in an infancy and has great potential. It is believed that with the popularization and application of the IoT, flexible energy harvesting devices will have broad application space when the problems and limitations are solved in the future.

Declaration of competing interest

The authors declare that they have no known competing financial interests or personal relationships that could have appeared to influence the work reported in this paper.

Data availability statement

Not applicable.

Acknowledgments

Author Contributions

All authors contributed to the study conception and design. Original draft writing was performed by Xiaoquan Shi, Dekai Li, Haitao Liu and Wenkun Xie. All authors commented on previous versions of the manuscript. The study was supervised by Yazhou Sun and Xichun Luo. All authors read and approved the final manuscript.

References

[1]   L Santos, B Cunha, I Fé, M Vieira, FA Silva (2021) Journal of Network and Systems Management 29. Doi:10.1007/s10922-021-09592-x

[2]   Q Shi, B Dong, T He, et al. (2020) InfoMat 2: 1131. Doi:10.1002/inf2.12122

[3]   G-T Hwang, V Annapureddy, JH Han, et al. (2016) Advanced Energy Materials 6. Doi:10.1002/aenm.201600237

[4]   T Buddhika, SL Pallickara, S Pallickara (2021) IEEE Transactions on Parallel and Distributed Systems 32: 2005. Doi:10.1109/tpds.2021.3055265

[5]   JJPC Rodrigues, DB De Rezende Segundo, HA Junqueira, et al. (2018) IEEE Access 6: 13129. Doi:10.1109/access.2017.2789329

[6]   S Wang, Y Jiang, H Tai, et al. (2019) Nano Energy 63. Doi:10.1016/j.nanoen.2019.06.025

[7]   Aaryashree, S Sahoo, P Walke, SK Nayak, CS Rout, DJ Late (2021) Nano Research 14: 3669. Doi:10.1007/s12274-021-3330-8

[8]   Z Wang, Z Gao (2020) Computational Intelligence 37: 1080. Doi:10.1111/coin.12337

[9]   J Shao, T Jiang, Z Wang (2020) Science China Technological Sciences 63: 1087. Doi:10.1007/s11431-020-1604-9

[10] MAP Mahmud, P Adhikary, A Zolfagharian, S Adams, A Kaynak, AZ Kouzani (2022) Electronic Materials Letters. Doi:10.1007/s13391-021-00327-3

[11] C Xu, Y Song, M Han, H Zhang (2021) Microsyst Nanoeng 7: 25. Doi:10.1038/s41378-021-00248-z

[12] H Ouyang, D Jiang, Y Fan, ZL Wang, Z Li (2021) Science Bulletin 66: 1709. Doi:10.1016/j.scib.2021.04.035

[13] AA Khan, MM Rana, G Huang, et al. (2020) Journal of Materials Chemistry A 8: 13619. Doi:10.1039/d0ta03416a

[14] I Dakua, N Afzulpurkar (2013) Nanomater Nanotechno 3. Doi:Artn 21

Doi 10.5772/56941

[15] AH Elsheikh, SW Sharshir, M Abd Elaziz, AE Kabeel, W Guilan, Z Haiou (2019) Solar Energy 180: 622. Doi:10.1016/j.solener.2019.01.037

[16] D Hao, L Qi, AM Tairab, et al. (2022) Renewable Energy 188: 678. Doi:10.1016/j.renene.2022.02.066

[17] Y Zhang, SJ Park (2019) Polymers (Basel) 11. Doi:10.3390/polym11050909

[18] L Tzounis, M Petousis, S Grammatikos, N Vidakis (2020) Materials (Basel) 13. Doi:10.3390/ma13122879

[19] M Xu, T Wu, Y Song, et al. (2021) Journal of Materials Chemistry C 9: 15552. Doi:10.1039/d1tc03886a

[20] H Su, X Wang, C Li, et al. (2021) Nano Energy 83. Doi:10.1016/j.nanoen.2021.105809

[21] CK Jeong, K-I Park, JH Son, et al. (2014) Energy Environ. Sci. 7: 4035. Doi:10.1039/c4ee02435d

[22] Z Chelli, H Achour, M Saidi, et al. (2021) Polymer-Plastics Technology and Materials: 1. Doi:10.1080/25740881.2021.1888995

[23] J Li, X Wang (2017) APL Mater 5. Doi:10.1063/1.4978936

[24] VA Cao, M Kim, W Hu, et al. (2021) ACS Nano 15: 10428. Doi:10.1021/acsnano.1c02757

[25] DH Kim, HJ Shin, H Lee, et al. (2017) Advanced Functional Materials 27. Doi:10.1002/adfm.201700341

[26] X Niu, W Jia, S Qian, et al. (2018) ACS Sustainable Chemistry & Engineering 7: 979. Doi:10.1021/acssuschemeng.8b04627

[27] Q Wu, H Guo, H Sun, X Liu, H Sui, F Wang (2021) Ceramics International 47: 19614. Doi:10.1016/j.ceramint.2021.03.299

[28] C Zhao, J Niu, Y Zhang, C Li, P Hu (2019) Composites Part B: Engineering 178. Doi:10.1016/j.compositesb.2019.107447

[29] G-T Hwang, J Yang, SH Yang, et al. (2015) Advanced Energy Materials 5. Doi:10.1002/aenm.201500051

[30] C Wang, X Gao, M Zheng, M Zhu, Y Hou (2021) ACS Appl Mater Interfaces 13: 41735. Doi:10.1021/acsami.1c12197

[31] C Dagdeviren, P Joe, OL Tuzman, et al. (2016) Extreme Mechanics Letters 9: 269. Doi:10.1016/j.eml.2016.05.015

[32] H Liu, J Zhong, C Lee, S-W Lee, L Lin (2018) Applied Physics Reviews 5. Doi:10.1063/1.5074184

[33] H Zhou, Y Zhang, Y Qiu, et al. (2020) Biosens Bioelectron 168: 112569. Doi:10.1016/j.bios.2020.112569

[34] F Narita, M Fox (2018) Advanced Engineering Materials 20. Doi:10.1002/adem.201700743

[35] Y Liu, L Wang, L Zhao, X Yu, Y Zi (2020) InfoMat 2: 318. Doi:10.1002/inf2.12079

[36] HS Kim, J-H Kim, J Kim (2011) International Journal of Precision Engineering and Manufacturing 12: 1129. Doi:10.1007/s12541-011-0151-3

[37] Z Yang, S Zhou, J Zu, D Inman (2018) Joule 2: 642. Doi:10.1016/j.joule.2018.03.011

[38] N Sezer, M Koç (2021) Nano Energy 80. Doi:10.1016/j.nanoen.2020.105567

[39] X Cao, Y Xiong, J Sun, X Zhu, Q Sun, ZL Wang (2021) Advanced Functional Materials. Doi:10.1002/adfm.202102983

[40] Z Zhao, Y Dai, SX Dou, J Liang (2021) Materials Today Energy 20. Doi:10.1016/j.mtener.2021.100690

[41] M Abbasipour, R Khajavi, AH Akbarzadeh (2022) Advanced Engineering Materials. Doi:10.1002/adem.202101312

[42] F Mokhtari, Z Cheng, R Raad, J Xi, J Foroughi (2020) Journal of Materials Chemistry A 8: 9496. Doi:10.1039/d0ta00227e

[43] GA Kaur, S Kumar, S Thakur, S Thakur, M Shandilya (2021) Journal of Materials Science: Materials in Electronics 32: 23631. Doi:10.1007/s10854-021-06854-x

[44] M Shandilya, R Rai, A Zeb (2017) Advances in Applied Ceramics 117: 255. Doi:10.1080/17436753.2017.1405557

[45] M Shandilya, S Thakur, R Rai (2019) Ferroelectrics Letters Section 46: 8. Doi:10.1080/07315171.2019.1647705

[46] W Deng, Y Zhou, A Libanori, G Chen, W Yang, J Chen (2022) Chem Soc Rev. Doi:10.1039/d1cs00858g

[47] A Gaur, S Tiwari, C Kumar, P Maiti (2020) Energy & Fuels 34: 6239. Doi:10.1021/acs.energyfuels.0c01143

[48] S Kumar, M Shandilya, S Thakur, N Thakur, G Anit Kaur (2019) Journal of Sol-Gel Science and Technology 92: 215. Doi:10.1007/s10971-019-05077-1

[49] KI Park, S Xu, Y Liu, et al. (2010) Nano Lett 10: 4939. Doi:10.1021/nl102959k

[50] CK Jeong, JH Lee, DY Hyeon, et al. (2020) Applied Surface Science 512. Doi:10.1016/j.apsusc.2019.144784

[51] D-J Shin, J Kim, J-H Koh (2018) Journal of the European Ceramic Society 38: 4395.
Doi:10.1016/j.jeurceramsoc.2018.05.022

[52] S Kumar, GA Kaur, A Saha, M Shandilya (2022) Didactic Transfer of Physics Knowledge through Distance Education: Didfyz 2021,

[53] B-Y Kim, W-H Lee, H-G Hwang, et al. (2016) Advanced Functional Materials 26: 5211.
Doi:10.1002/adfm.201505569

[54] SS Won, M Kawahara, CW Ahn, et al. (2019) Advanced Electronic Materials 6. Doi:10.1002/aelm.201900950

[55] W Qin, P Zhou, Y Qi, T Zhang (2020) Micromachines (Basel) 11. Doi:10.3390/mi11110966

[56] S Kumar, M Shandilya, S Thakur, N Thakur (2018) Journal of Sol-Gel Science and Technology 88: 646.
Doi:10.1007/s10971-018-4791-y

[57] M Shandilya, R Rai, A Zeb, S Kumar (2017) Ferroelectrics 520: 93. Doi:10.1080/00150193.2017.1375323

[58] S Kumar, M Shandilya, Ga Kaur, N Thakur (2022) Bulletin of Materials Science 45. Doi:10.1007/s12034-021-02606-z

[59] S Xu, G Poirier, N Yao (2012) Nano Lett 12: 2238. Doi:10.1021/nl204334x

[60] Y Zhang, L Zhou, X Gao, et al. (2021) Nano Energy 89. Doi:10.1016/j.nanoen.2021.106319

[61] HY Choi, YG Jeong (2019) Composites Part B: Engineering 168: 58. Doi:10.1016/j.compositesb.2018.12.072

[62] W Liu, X Ren (2009) Phys Rev Lett 103: 257602. Doi:10.1103/PhysRevLett.103.257602

[63] MP Aleksandrova, TD Tsanev, IM Pandiev, GH Dobrikov (2020) Energy 205.
Doi:10.1016/j.energy.2020.118068

[64] Y Wang, Q Zhang, L Hu, E Yu, H Yang (2016) Journal of Alloys and Compounds 685: 1.
Doi:10.1016/j.jallcom.2016.05.265

[65] SS Ham, G-J Lee, DY Hyeon, et al. (2021) Composites Part B: Engineering 212.
Doi:10.1016/j.compositesb.2021.108705

[66] Z-H Zhao, M-Y Ye, H-M Ji, X-L Li, X Zhang, Y Dai (2018) Materials & Design 137: 184.
Doi:10.1016/j.matdes.2017.10.003

[67] K Batra, N Sinha, B Kumar (2019) Journal of Materials Science: Materials in Electronics 30: 6157.
Doi:10.1007/s10854-019-00917-w

[68] ZL Wang, JH Song (2006) Science 312: 242. Doi:10.1126/science.1124005

[69] KH Kim, KY Lee, JS Seo, B Kumar, SW Kim (2011) Small 7: 2577. Doi:10.1002/smll.201100819

[70] P He, W Chen, J Li, H Zhang, Y Li, E Wang (2020) Science Bulletin 65: 35. Doi:10.1016/j.scib.2019.09.026

[71] L Algieri, MT Todaro, F Guido, et al. (2018) ACS Applied Energy Materials. Doi:10.1021/acsaem.8b00820

[72] W Zhang, H Yang, L Li, et al. (2020) Nanotechnology 31: 385401. Doi:10.1088/1361-6528/ab991f

[73] RA Street, TN Ng, RA Lujan, et al. (2014) ACS Appl Mater Interfaces 6: 4428. Doi:10.1021/am500126b

[74] I Choudhary, Deepak (2021) Journal of Materials Science: Materials in Electronics 32: 7875.
Doi:10.1007/s10854-021-05512-6

[75] MA Franco, PP Conti, RS Andre, DS Correa (2022) Sensors and Actuators Reports 4.
Doi:10.1016/j.snr.2022.100100

[76] Z Rafiee, A Mosahebfard, MH Sheikhi (2020) Materials Science in Semiconductor Processing 115. Doi:10.1016/j.mssp.2020.105116

[77] S Roa, M Sandoval, MJC Burgos, P Manidurai, S Suárez (2021) Journal of Alloys and Compounds 871. Doi:10.1016/j.jallcom.2021.159559

[78] I Choudhary, R Shukla, A Sharma, KK Raina (2020) Journal of Materials Science: Materials in Electronics 31: 20033. Doi:10.1007/s10854-020-04525-x

[79] K Batra, N Sinha, B Kumar (2020) Ceramics International 46: 24120. Doi:10.1016/j.ceramint.2020.06.191

[80] M Aleksandrova (2020) Microelectronic Engineering 233. Doi:10.1016/j.mee.2020.111434

[81] A Apte, K Mozaffari, FS Samghabadi, et al. (2020) Adv Mater 32: e2000006. Doi:10.1002/adma.202000006

[82] W Wu, L Wang, Y Li, et al. (2014) Nature 514: 470. Doi:10.1038/nature13792

[83] P Li, Z Zhang, W Shen, C Hu, W Shen, D Zhang (2021) Journal of Materials Chemistry A 9: 4716. Doi:10.1039/d0ta10457d

[84] MB Ghasemian, T Daeneke, Z Shahrbabaki, J Yang, K Kalantar-Zadeh (2020) Nanoscale 12: 2875. Doi:10.1039/c9nr08063e

[85] GT Hwang, H Park, JH Lee, et al. (2014) Adv Mater 26: 4880. Doi:10.1002/adma.201400562

[86] Y Manjula, R Rakesh Kumar, PM Swarup Raju, et al. (2020) Chemical Physics 533. Doi:10.1016/j.chemphys.2020.110699

[87] CS Lee, J Joo, S Han, SK Koh (2004) Applied Physics Letters 85: 1841. Doi:10.1063/1.1784890

[88] A Gaur, R Shukla, B Kumar, et al. (2016) Polymer 97: 362. Doi:10.1016/j.polymer.2016.05.049

[89] Z Pi, J Zhang, C Wen, Z-b Zhang, D Wu (2014) Nano Energy 7: 33. Doi:10.1016/j.nanoen.2014.04.016

[90] K Ibtehaj, MH Hj Jumali, S Al-Bati (2020) Polymer 208. Doi:10.1016/j.polymer.2020.122956

[91] Z Liu, S Zhang, YM Jin, et al. (2017) Semiconductor Science and Technology 32. Doi:10.1088/1361-6641/aa68d1

[92] MA Barique, Y Neo, M Noyori, L Aprila, M Asai, H Mimura (2021) Nanotechnology 32: 015401. Doi:10.1088/1361-6528/abb5d3

[93] S Kim, I Towfeeq, Y Dong, S Gorman, A Rao, G Koley (2018) Applied Sciences 8. Doi:10.3390/app8020213

[94] JS Xiaoliang Chen, Yucheng Ding, Hongmiao Tian, Xiangming Li, Yaopei Zhou (2015).

[95] X Chen, H Tian, X Li, et al. (2015) Nanoscale 7: 11536. Doi:10.1039/c5nr01746g

[96] H Kawai (1969) Japanese Journal of Applied Physics 8: 975.

[97] B Baytekin, HT Baytekin, BA Grzybowski (2013) Energy & Environmental Science 6. Doi:10.1039/c3ee41360h

[98] L Lu, W Ding, J Liu, B Yang (2020) Nano Energy 78. Doi:10.1016/j.nanoen.2020.105251

[99] DM Correia, J Nunes-Pereira, D Alikin, et al. (2019) Polymer 169: 138. Doi:10.1016/j.polymer.2019.02.042

[100] P Martins, AC Lopes, S Lanceros-Mendez (2014) Progress in Polymer Science 39: 683. Doi:10.1016/j.progpolymsci.2013.07.006

[101] A Salimi, AA Yousefi (2003) Polymer Testing 22: 699. Doi:10.1016/s0142-9418(03)00003-5

[102] J Gomes, J Serrado Nunes, V Sencadas, S Lanceros-Mendez (2010) Smart Materials and Structures 19. Doi:10.1088/0964-1726/19/6/065010

[103] L Li, M Zhang, M Rong, W Ruan (2014) RSC Adv. 4: 3938. Doi:10.1039/c3ra45134h

[104]   Y Zhou, J Liu, X Hu, DR Salem, B Chu (2019) Applied Physics Express 12. Doi:10.7567/1882-0786/ab207b

[105]   R Senthil Kumar, T Sarathi, KK Venkataraman, A Bhattacharyya (2019) Materials Letters 255. Doi:10.1016/j.matlet.2019.126515

[106]   K Roy, D Mandal (2018),

[107]   S Chen, K Yao, FEH Tay, CL Liow (2007) Journal of Applied Physics 102. Doi:10.1063/1.2812702

[108]   MMD Ramos, HMG Correia, S Lanceros-Méndez (2005) Computational Materials Science 33: 230. Doi:10.1016/j.commatsci.2004.12.041

[109]   S Ojha, S Paria, SK Karan, et al. (2019) Nanoscale 11: 22989. Doi:10.1039/c9nr08315d

[110]   T Soulestin, V Ladmiral, FD Dos Santos, B Améduri (2017) Progress in Polymer Science 72: 16. Doi:10.1016/j.progpolymsci.2017.04.004

[111]   PH Ducrot, I Dufour, C Ayela (2016) Sci Rep 6: 19426. Doi:10.1038/srep19426

[112]   D Singh, A Choudhary, A Garg (2018) ACS Appl Mater Interfaces 10: 2793. Doi:10.1021/acsami.7b16973

[113]   C Lee, JA Tarbutton (2014) Smart Materials and Structures 23. Doi:10.1088/0964-1726/23/9/095044

[114]   J Yu, K Cai, L Jin, et al. (2019) Nanoscale 11: 14896. Doi:10.1039/c9nr05427h

[115]   V Sencadas (2020) ACS Applied Polymer Materials 2: 2105. Doi:10.1021/acsapm.0c00209

[116]   J Zhu, L Jia, R Huang (2017) Journal of Materials Science: Materials in Electronics 28: 12080. Doi:10.1007/s10854-017-7020-5

[117]   BY Lee, J Zhang, C Zueger, et al. (2012) Nat Nanotechnol 7: 351. Doi:10.1038/nnano.2012.69

[118]   MM Alam, D Mandal (2016) ACS Appl Mater Interfaces 8: 1555. Doi:10.1021/acsami.5b08168

[119]   JH Lee, JH Lee, J Xiao, MS Desai, X Zhang, SW Lee (2019) Nano Lett 19: 2661. Doi:10.1021/acs.nanolett.9b00569

[120]   SK Ghosh, D Mandal (2016) Nano Energy 28: 356. Doi:10.1016/j.nanoen.2016.08.030

[121]   N Chamankar, R Khajavi, AA Yousefi, A Rashidi, F Golestanifard (2020) Ceramics International 46: 23567. Doi:10.1016/j.ceramint.2020.06.128

[122]   X Song, L He, W Yang, et al. (2019) Journal of Manufacturing Science and Engineering 141. Doi:10.1115/1.4044708

[123]   H Kim, C Sohn, G-T Hwang, K-I Park, CK Jeong (2020) Journal of the Korean Ceramic Society 57: 401. Doi:10.1007/s43207-020-00038-9

[124]   Y Zhuang, Z Xu, F Li, Z Liao, W Liu (2015) Journal of Alloys and Compounds 629: 113. Doi:10.1016/j.jallcom.2014.12.239

[125]   CC Jin, CH Liu, XC Liu, Y Wang, HL Hwang (2018) Ceramics International 44: 17391. Doi:10.1016/j.ceramint.2018.06.204

[126]   Z Wang, F Narita (2019) Advanced Engineering Materials 21. Doi:10.1002/adem.201900169

[127]   Z Wang, F Narita (2019) Journal of Applied Physics 126. Doi:10.1063/1.5127937

[128]   KT Arul, M Ramanjaneyulu, MS Ramachandra Rao (2019) Current Applied Physics 19: 375. Doi:10.1016/j.cap.2019.01.003

[129]   MH Malakooti, F Jule, HA Sodano (2018) ACS Appl Mater Interfaces 10: 38359. Doi:10.1021/acsami.8b13643

[130]   J-I Park, G-Y Lee, J Yang, C-S Kim, S-H Ahn (2015) Journal of Composite Materials 50: 1573. Doi:10.1177/0021998315577685

[131]   X Gao, M Zheng, X Yan, J Fu, Y Hou, M Zhu (2020) Nanoscale 12: 5175. Doi:10.1039/d0nr00111b

[132]   J Shi, SP Beeby (2020) 2019 19th International Conference on Micro and Nanotechnology for Power Generation and Energy Conversion Applications (Powermems). Doi:10.1109/PowerMEMS49317.2019.71805303905

[133]   K Shi, B Sun, X Huang, P Jiang (2018) Nano Energy 52: 153. Doi:10.1016/j.nanoen.2018.07.053

[134]   CT Pan, SY Wang, CK Yen, et al. (2020) ACS Omega 5: 17090. Doi:10.1021/acsomega.0c00805

[135]   R Sahoo, S Mishra, L Unnikrishnan, et al. (2020) Materials Science in Semiconductor Processing 117. Doi:10.1016/j.mssp.2020.105173

[136]   H Kim, F Torres, D Villagran, C Stewart, Y Lin, T-LB Tseng (2017) Macromolecular Materials and Engineering 302. Doi:10.1002/mame.201700229

[137]   CK Jeong, C Baek, AI Kingon, KI Park, SH Kim (2018) Small 14: e1704022. Doi:10.1002/smll.201704022

[138]   G Jian, Y Jiao, Q Meng, H Shao, F Wang, Z Wei (2020) Advanced Materials Interfaces 7. Doi:10.1002/admi.202000484

[139]   A Waseem, MA Johar, MA Hassan, et al. (2021) Journal of Alloys and Compounds 860. Doi:10.1016/j.jallcom.2020.158545

[140]   S Bairagi, SW Ali (2020) Organic Electronics 78. Doi:10.1016/j.orgel.2019.105547

[141]   SH Shin, SY Choi, MH Lee, J Nah (2017) ACS Appl Mater Interfaces 9: 41099. Doi:10.1021/acsami.7b11773

[142]   NR Alluri, A Chandrasekhar, V Vivekananthan, et al. (2017) ACS Sustainable Chemistry & Engineering 5: 4730. Doi:10.1021/acssuschemeng.7b00117

[143]   T Gao, J Liao, J Wang, et al. (2015) Journal of Materials Chemistry A 3: 9965. Doi:10.1039/c5ta01079a

[144]   N Chamankar, R Khajavi, AA Yousefi, A Rashidi, F Golestanifard (2020) Ceramics International 46: 19669. Doi:10.1016/j.ceramint.2020.03.210

[145]   GA Kaur, S Kumar, M Shandilya (2020) Journal of Materials Science: Materials in Electronics. Doi:10.1007/s10854-020-04550-w

[146]   S Siddiqui, D-I Kim, E Roh, et al. (2016) Nano Energy 30: 434. Doi:10.1016/j.nanoen.2016.10.034

[147]   C Wang, M Zheng, X Gao, J Fu, M Zhu, Y Hou (2020) European Journal of Inorganic Chemistry 2020: 770. Doi:10.1002/ejic.202000003

[148]   C Hu, L Cheng, Z Wang, Y Zheng, S Bai, Y Qin (2016) Small 12: 1315. Doi:10.1002/smll.201502453

[149]   M Gao, L Li, W Li, H Zhou, Y Song (2016) Adv Sci (Weinh) 3: 1600120. Doi:10.1002/advs.201600120

[150]   A Nafari, HA Sodano (2019) Smart Materials and Structures 28. Doi:10.1088/1361-665X/aadb6c

[151]   CC Jin, HH Fan, Y Wang, HL Hwang, YF Zhang, Q Wang (2017) Ceramics International 43: 14476. Doi:10.1016/j.ceramint.2017.06.112

[152]   D Dhakras, S Ogale (2016) Advanced Materials Interfaces 3. Doi:10.1002/admi.201600492

[153]   SI Jeong, EJ Lee, GR Hong, et al. (2020) ACS Omega 5: 1956. Doi:10.1021/acsomega.9b03753

[154]   H Guo, Q Wu, H Sun, X Liu, H Sui (2020) Materials Today Energy 17. Doi:10.1016/j.mtener.2020.100489

[155]   Y Yang, H Pan, G Xie, et al. (2020) Sensors and Actuators A: Physical 301. Doi:10.1016/j.sna.2019.111789

[156]   X Guan, B Xu, J Gong (2020) Nano Energy 70. Doi:10.1016/j.nanoen.2020.104516

[157]   Z-H Dai, T Li, Y Gao, et al. (2018) Colloids and Surfaces A: Physicochemical and Engineering Aspects 548: 179. Doi:10.1016/j.colsurfa.2018.03.056

[158]   Y Fan, X Huang, G Wang, P Jiang (2015) The Journal of Physical Chemistry C 119: 27330. Doi:10.1021/acs.jpcc.5b09619

[159]   Z Zhou, Z Zhang, Q Zhang, et al. (2020) ACS Appl Mater Interfaces 12: 1567. Doi:10.1021/acsami.9b18780

[160]   C Baek, JH Yun, JE Wang, et al. (2016) Nanoscale 8: 17632. Doi:10.1039/c6nr05784e

[161]   D-J Shin, J-H Ji, J Kim, GH Jo, S-J Jeong, J-H Koh (2019) Journal of Alloys and Compounds 802: 562. Doi:10.1016/j.jallcom.2019.05.363

[162]   V Sharma, G Anit Kaur, N Gupta, M Shandilya (2020) FlatChem 24. Doi:10.1016/j.flatc.2020.100195

[163]   N Gupta, G Kaur, V Sharma, R Nagraik, M Shandilya (2022) Journal of Electroanalytical Chemistry 904. Doi:10.1016/j.jelechem.2021.115904

[164]   GA Kaur, V Sharma, N Gupta, M Shandilya, R Rai (2021) Materials Letters 304. Doi:10.1016/j.matlet.2021.130616

[165]   MFL De Volder, SH Tawfick, RH Baughman, AJ Hart (2013) Science 339: 535. Doi:10.1126/science.1222453

[166]   K-I Park, M Lee, Y Liu, et al. (2012) Advanced Materials 24: 2999. Doi:10.1002/adma.201200105

[167]   A Anand, D Meena, MC Bhatnagar (2020) Journal of Alloys and Compounds 843. Doi:10.1016/j.jallcom.2020.156019

[168]   V Vivekananthan, NR Alluri, Y Purusothaman, A Chandrasekhar, SJ Kim (2017) Nanoscale 9: 15122. Doi:10.1039/c7nr04115b

[169]   Y Sun, J Chen, X Li, Y Lu, S Zhang, Z Cheng (2019) Nano Energy 61: 337. Doi:10.1016/j.nanoen.2019.04.055

[170]   V Vivekananthan, A Chandrasekhar, NR Alluri, et al. (2019) Materials Letters 249: 73. Doi:10.1016/j.matlet.2019.02.134

[171]   Y Wang, X Zhang, X Guo, et al. (2018) Journal of Materials Science 53: 13081. Doi:10.1007/s10853-018-2540-9

[172]   F Ram, K Suresh, A Torris, G Kumaraswamy, K Shanmuganathan (2021) Ceramics International 47: 15750. Doi:10.1016/j.ceramint.2021.02.147

[173]   HJ Choi, YS Jung, J Han, YS Cho (2020) Nano Energy 72. Doi:10.1016/j.nanoen.2020.104735

[174]   HB Kang, CS Han, JC Pyun, WH Ryu, C-Y Kang, YS Cho (2015) Composites Science and Technology 111: 1. Doi:10.1016/j.compscitech.2015.02.015

[175]   H Kim, F Torres, MT Islam, et al. (2017) MRS Communications 7: 960. Doi:10.1557/mrc.2017.126

[176]   X Chen, X Li, J Shao, et al. (2017) Small 13. Doi:10.1002/smll.201604245

[177]   CR Bowen, DN Betts, HA Kim, V Yu. Topolov (2013) Microsystem Technologies 20: 709. Doi:10.1007/s00542-013-2012-8

[178]   Z Zeng, L Gai, X Wang, et al. (2017) Applied Physics Letters 110. Doi:10.1063/1.4977938

[179]   Y Hao, Y Hou, J Fu, et al. (2020) Nanoscale 12: 13001. Doi:10.1039/d0nr03056b

[180]   Y Zhang, CK Jeong, J Wang, et al. (2018) Nano Energy 50: 35. Doi:10.1016/j.nanoen.2018.05.025

[181]   Z Wang, X Yuan, J Yang, et al. (2020) Nano Energy 73. Doi:10.1016/j.nanoen.2020.104737

[182]   A Chortos, Z Bao (2014) Mater Today 17: 321. Doi:10.1016/j.mattod.2014.05.006

[183]   X Zhou, K Parida, O Halevi, et al. (2020) Nano Energy 72. Doi:10.1016/j.nanoen.2020.104676

[184]   M Aleksandrova, T Ivanova, F Hamelmann, V Strijkova, K Gesheva (2020) Coatings 10.
         Doi:10.3390/coatings10070650

[185]   MG Kang, SM Oh, WS Jung, et al. (2015) Sci Rep 5: 10151. Doi:10.1038/srep10151

[186]   Q Zhou, S Lau, D Wu, KK Shung (2011) Prog Mater Sci 56: 139. Doi:10.1016/j.pmatsci.2010.09.001

[187]   C Jin, N Hao, Z Xu, et al. (2020) Sensors and Actuators A: Physical 305. Doi:10.1016/j.sna.2020.111912

[188]   H Kozuka, M Kajimura (2000) J Am Ceram Soc 83: 1056.

[189]   M Koç, L Paralı, O Şan (2020) Polymer Testing 90. Doi:10.1016/j.polymertesting.2020.106695

[190]   R Atif, J Khaliq, M Combrinck, et al. (2020) Polymers (Basel) 12. Doi:10.3390/polym12061304

[191]   PK Szewczyk, A Gradys, SK Kim, et al. (2020) ACS Appl Mater Interfaces 12: 13575.
         Doi:10.1021/acsami.0c02578

[192]   C Chen, X Wang, Y Wang, et al. (2020) Advanced Functional Materials 30. Doi:10.1002/adfm.202005141

[193]   H Kim, J Johnson, LA Chavez, CA Garcia Rosales, T-LB Tseng, Y Lin (2018) Ceramics International 44:
         9037. Doi:10.1016/j.ceramint.2018.02.107